STATE HIGHWAY ADMINISTRATION

RESEARCH REPORT

Volume II

INFLUENCE OF FINE AGGREGATE LITHOLOGY ON DELAYED ETTRINGITE FORMATION IN HIGH EARLY STRENGTH CONCRETE

The University of Maryland
In Collaboration with the Federal Highway Administration

MD-04-SP107B4U
FINAL REPORT

July 2004

Technical Report Documentation Page

1. Report No.	2. Government Accession No.	3. Recipient's Catalog No.
MD-04-SP107B4U		

4. Title and Subtitle	5. Report Date
Influence of Fine Aggregate Lithology on Delayed Ettringite Formation in High Early Strength Concrete	July 2004
	6. Performing Organization Code

7. Author/s	8. Performing Organization Report No.
A.M. Amde, K. Williams and R.A. Livingston	

9. Performing Organization Name and Address	10. Work Unit No. (TRAIS)
Dept of Civil and Environmental Engineering **University of Maryland** College Park, M D 2074 2	11. Contract or Grant No. SP107B4U

12. Sponsoring Organization Name and Address	13. Type of Report and Period Covered
Maryland State Highway Administration Office of Policy & Research 707 North Calvert Street Baltimore MD 21202	Final Report
	14. Sponsoring Agency Code

15. Supplementary Notes
This project was performed in cooperation with the Federal Highway Administration

16. Abstract

The study investigated the influence of Maryland fine aggregates on delayed ettringite formation (DEF). The main variable in the study was MDSHA expansion test rating of the fine aggregates, which is used as a surrogate for ASR reactivity. The scope of the study was limited to three fine aggregates currently being used in Maryland State Highway projects: Millville, Brandywine, and Silver Hill. Only one coarse aggregate, non-reactive Frederick limestone was used throughout the study and all other concrete mix factors were kept constant. Two replicate sets of prisms were involved; one set stored under water, the other in 100% RH. Also, as a control, a third set of Millville specimens was stored under dry, i.e. ambient RH, conditions. The Duggan test as modified by UMD/FHWA, SEM with EDXRD, and X-ray Computed Tomography were used to investigate DEF as the possible damage mechanism. In addition, compressive strength was measured at 28 days and 270 days.

This study concludes that fine aggregate type can significantly predispose a concrete sample to DEF and associated damaging expansion, while the exposure condition may exacerbate the effect. For example, the samples made from the sand with the highest MDSHA rating, Silver Hill, and stored under water exhibited the most ettringite and had the most severe expansion in terms of rate, duration, and amount. Additionally, water exposure seemed to enable DEF.

The expansions observed in this research program agreed with the ranking obtained in the MDSHA test: Silver Hill was the highest, Brandywine intermediate and Millville, the crushed limestone, the lowest. However, for the two siliceous aggregate types the expansion measurements did not predict the correct rank order of damage as measured by compressive strength at 270 days. The kinetics of the expansion varied among the aggregates. It is important to examine the expansion rate curve, i.e. the time derivative of expansion, to characterize the process rather than relying solely on the measured expansion at some fixed point in time. The various aggregates showed different responses to fog vs. submerged conditions. This suggests that the effect of each type of aggregate on the microstructure and hence the absorptivity of the cement paste needs to be considered in addition to its potential for ASR in evaluating expansion test data.

Ettringite was observed in most of the specimens. The morphology of the crystals may be an indication of the progress of damage. However, there is no quantitative way of correlating DEF with expansion measurements at the present time. Finally, the results show that the measured expansions come from a combination of moisture absorption, DEF and ASR. Consequently, expansion tests do not measure ASR effects only.

17. Key Words	18. Distribution Statement: No restrictions
Ettringite, ASR, Delayed Ettringite Formation, Fine Aggregate, Expansion	This document is available from the Research Division upon request.

19. Security Classification (of this report)	20. Security Classification (of this page)	21. No. of Pages	22. Price
None	None	113	

Form DOT F 1700.7 (8-72) Reproduction of form and completed page is authorized.

ABSTRACT

INFLUENCE OF FINE AGGREGATE LITHOLOGY ON DELAYED ETTRINGITE FORMATION IN HIGH EARLY STRENGTH CONCRETE

The study investigated the influence of Maryland fine aggregates on delayed ettringite formation (DEF). The main variable in the study was MDSHA expansion test rating of the fine aggregates, which is used as a surrogate for ASR reactivity. The scope of the study was limited to three fine aggregates currently being used in Maryland State Highway projects: Millville, Brandywine, and Silver Hill. Only one coarse aggregate, non-reactive Frederick limestone was used throughout the study and all other concrete mix factors were kept constant. Two replicate sets of prisms were involved; one set stored under water, the other in 100% relative humidity (RH). Also, as a control, a third set of Millville specimens was stored under dry, i.e. ambient RH, conditions. The Duggan test as modified by UMD/FHWA, SEM with EDXRD, and X-ray Computed Tomography were used to investigate DEF as the possible damage mechanism. In addition, compressive strength was measured at 28 days and 270 days.

This study concludes that fine aggregate type can significantly predispose a concrete sample to DEF and associated damaging expansion, while the exposure condition may exacerbate the effect. For example, the samples made from the sand with the highest MDSHA rating, Silver Hill, and stored under water exhibited the most ettringite and had the most severe expansion in terms of rate, duration, and amount. Additionally, water exposure seemed to enable DEF. For example, concrete samples made with Millville sand and stored under water were commonly found with various forms of ettringite, while dry samples of the same type had little or no ettringite.

The expansions observed in this research program agreed with the ranking obtained in the MDSHA test: Silver Hill was the highest, Brandywine intermediate and Millville, the crushed limestone, the lowest. However, for the two siliceous aggregate types the expansion measurements did not predict the correct rank order of damage as measured by compressive strength at 270 days. The kinetics of the expansion varied among the aggregates. It is important to examine the expansion rate curve, i.e. the time derivative of expansion, to characterize the process rather than relying solely on the measured expansion at some fixed point in time. The various aggregates showed different responses to fog vs. submerged conditions. This suggests that the effect of each type of aggregate on the microstructure and hence the absorptivity of the cement paste needs to be considered in addition to its potential for ASR in evaluating expansion test data.

Ettringite was observed in most of the specimens. The morphology of the crystals may be an indication of the progress of damage. However, there is no quantitative way of correlating DEF with expansion measurements at the present time. Finally, the results show that the measured expansions come from a combination of moisture absorption, DEF and ASR. Consequently, expansion tests do not measure ASR effects only.

ACKNOWLEDGEMENTS

The research reported herein was sponsored by the Maryland State Highway Administration (MDSHA). Sincere thanks are due to Mr. Earle S. Freedman, Deputy Chief Engineer of Bridge Development, MDSHA; Mr. Peter Stephanos, Director of Materials and Technology, MDSHA; and Mr. Jeffrey H. Smith, Chief, Research Division, MDSHA, for their guidance and support. The authors are very grateful to Mr. Paul Finnerty, Office of Materials and Technology, Precast/Prestressed Concrete Division, MDSHA, for his technical advice and support throughout the project and for coordinating and administrating support from the state of Maryland. The authors also appreciate the support provided by Ms. Barbara Adkins, MDSHA; and by Ms. Vicki Stewart, MDSHA.

The project is very grateful to Dr. W. Clayton Ormsby, Research Chemist, Salut, Inc., for the help and expertise provided on the Scanning Electron Microscope work; to Dr. Habeeb Saleh, Senior Scientist, WJE Associates, Inc., NDE Validation Center, for the expertise he provided in Computed Tomography) X-ray; and to Dr. Marcia Simon for her help and advice on the laboratory work performed at FHWA.

Appreciations are also due to Mr. Gary M. Mullings, Director of Operations & Compliance, National Ready Mixed Concrete Association (NRMCA); and Mr. Solimon Ben-Barka, Laboratory Technician, NRMCA, for helping with the preparation and testing of concrete samples at the Smith Joint Research Laboratory in College Park, MD.

Aggregate Industries Management Inc., US Corporate Office, donated over two tons of raw materials for this research. Mr. Indra Kumar, Aggregate Industries Lab, Mid – Atlantic region, was helpful in selecting the fine aggregates. The authors would also like to acknowledge former graduate student at University of Maryland, Dr. Amal Azzam, for her advice and support and to Mr. Tsegahum Tessema & the staff of the PCCP lab, Federal Highway Administration, for help with the design and mixing of concrete batches.

TABLE OF CONTENTS

LIST OF FIGURES

LIST OF TABLES

CHAPTER 1- Introduction

A potentially serious deterioration problem in concrete is associated with delayed ettringite formation (DEF). Many countries have reported deterioration of concrete structures where the main cause of distress has been identified as DEF. In 2000, it was reported that 375 out of 860 precast elements of Brewer Stadium, North Carolina, in the United States showed severe cracking and spalling. In addition, 100 precast elements were slightly deteriorated. The cracks and spalling started only after eight years of construction and the main mechanism of deterioration identified was distress caused by DEF. The reconstruction of the stadium was chosen as the most economical solution. In 1995 the Texas Department of Transportation found significant cracks in 56 precast concrete beams waiting installation in highway bridges. Analysis indicated that the damage appeared to be caused by DEF. The beams were written off at a cost of U.S. $250,000. Other countries that have reported damage include South Africa, Egypt, United Kingdom, Germany and Scandinavia.

1.1 The Mineral Ettringite

Ettringite is a complex mineral that forms in cement pastes from reaction between calcium, aluminum and sulfate. Pure ettringite has the chemical formula:

$$3\,CaO\,Al_2O_3\,3CaSO_4\,32H_2O$$

or in cement chemists notation,

$$C_6\,A\,S_3\,H_{32}$$

Ettringite naturally forms during the early hydration process of cement, while the concrete is still plastic. Its formation greatly influences many properties of concretes made from Portland cement, such as setting of cement, strength, durability, etc. However, the early type of ettringite is harmless and does not produce any damage. The early ettringite decomposes, but in some cases, it may reform at a later stage, after months or years, a process, which is called, delayed ettringite formation (DEF). Sometimes it is also referred to as secondary ettringite formation. It is generally believed that DEF formation

can cause expansion and deterioration of concrete. DEF damage is typically viewed as the result of an expansive process within the material similar to that of alkali-silicate reaction (ASR), but many aspects of this process remain controversial.

1.2 Formation of Ettringite During Cement Hydration

Cement hydration is driven by the reactions of water molecules with the cement's constituents (C_3S, C_2S, C_4A, C_4AF) (See Table 1.1). These reactions commonly proceed in the presence of gypsum and proprietary additives designed to alter the properties of the resulting concrete. Generally, the reactions proceed in sequence. For example, tricalcium aluminate (C_3A) hydrates first with gypsum to produce ettringite and heat. The resulting ettringite then may participate in subsequent reactions to produce monosulfoaluminate.

The primary products of cement hydration are calcium silicate hydrate (C – S – H), calcium hydroxide (CH), and ettringite. The formation of ettringite is accompanied by a volumetric expansion of the concrete matrix. During its initial formation, the associated volume increase does not result in distress since it occurs while the cement is in a plastic and in a porous state (wet cement).

1.3 Delayed Ettringite Formation (DEF)

After curing, concrete remains a highly reactive material and it continues to change chemically and physically as its constituents interact with the external environment. Often these changes degrade the overall integrity of the concrete. The extent and severity of any physical or chemical change is influenced by the exposure conditions of the concrete.

Some common mechanisms enabling the deterioration of concrete are reinforcement corrosion and expansion, weathering, alkali-silica reaction (ASR), and sulfate attack. Delayed ettringite formation is considered to be the result of an internal sulfate attack since it requires no source of sulfate from the

surrounding environment. There are two models commonly used to explain the occurrence of DEF in concrete.

1.4 DEF: Thermal Decomposition Model

Internal sulfate attack and the DEF it triggers may be a symptom of improper heat or steam curing of the concrete. Thus, the thermal decomposition model is best applied to prefabricated steam cured concrete members that may have been exposed to excessively high temperatures. Under this model, ettringite formation in cement materials is suppressed at temperatures elevated above 70_o C [Lawrence, 1995; Ronne and Sellevold, 1994]. This results in a high concentration of sulfate in the pore liquid of the hardened cement paste. The sulfate is free to combine with calcium and aluminum containing constituents of the cement paste to produce ettringite.

This secondary or delayed formation of ettringite is accompanied by damaging expansion of the cement paste. As the expansion advances, the cement paste tends to separate from the coarse aggregate forming gaps in the concrete matrix. DEF can be diagnosed by the presence of gaps completely encircling the coarse aggregate. With time these gaps can become filled with ettringite.

1.5 DEF: Holistic Approach Model

As pointed out by Collepardi et al [1999], the main shortfall of the thermal decomposition model is that it fails to explain the occurrence of DEF in all concrete members. Specifically those that have no history of heat treatment, steam curing, or exposure to excessively high temperatures (i.e. $>70^0$ C).

Collepardi has subsequently introduced an alternative model that can be applied to all concrete members. This holistic approach model postulates that the risk of DEF due to internal sulfate attack is greatest whenever three necessary

conditions are met. The three critical conditions are micro cracking, late sulfate release, and exposure to water.

There are several causes for micro cracks in a concrete member including dynamic service loads, freeze/thaw cycles, plastic shrinkage, and ASR. Under the holistic approach model, the micro-cracks are pre-existing, that is, they occur before the onset of DEF. The micro-cracks provide a space for the accumulation of ettringite. It is here noted that capillary voids as well as entrained air can also provide space for ettringite deposition.

Portland cement contains several forms of sulfate with varying degrees of reactivity. For instance, the common sulfate gypsum is soluble and would hydrate relatively quickly. Generally, gypsum would not be available for secondary ettringite formation.

Sulfates in Portland cement with lower solubility have been suspected as the source of the late sulfate release. Sulfates in the clinker phase of the cement may remain in the hardened cement due to its low solubility, but may hydrate later to form secondary ettringite.

Miller and Tang et al [1996] studied sulfate in cement clinker using samples from a large number of North American cement producers. Four common sulfates where found in the clinker: Arcanite (K_2SO_4), Aphthitalite ($3K_2SO_4 – Na_2SO_4$), Calcium Langbeinite ($2CaSO_4 – K_2SO_4$), and Belite (chiefly from silicates). The presence of these sulfates are explained by the use of sulfur rich fuels burned in cement kilns such as coal fuel, oil and old rubber tires.

Water is responsible for the migration of reactant ions (SO_4^{2+}, $Al(OH)^{4-}$, and Ca^{2+}) to the sites of micro-cracks [Collepardi, 1999]. The ions feed the growth of the ettringite crystals, which in turn expand and widen the cracks.

Alternating moisture conditions such as wetting and drying cycles can further facilitate the migration process by producing gradients between the concrete and its surroundings. Internally, gradients in moisture can produce a

highly dynamic system in which cement phase constituents and water-soluble alkalis are moved until equilibrium is reached. Recently, Thomas (2002) has criticized the holistic model as not being truly holistic because it omits several other important factors.

1.6 The Connection Between ASR and DEF

Alkali-Silica Reaction (ASR) and Delayed Ettringite Formation (DEF) crystal are often observed together. In fact, sometimes the two are confused though DEF can be easily distinguished from ASR by crystal morphology and chemistry. However, this identification requires destructive sampling. Instead, the presence of ASR or DEF is often simply inferred from the visual evidence of expansive map cracking, which can lead to misdiagnosis.

ASR is the product of the interaction of potassium or sodium ions released from cement compounds and reactive silica in the aggregates, whereas DEF is a form of internal sulfate attack. Thus, ASR and DEF are separate and distinct chemical processes. If there is a connection, it may be that in some cases the hairline cracks caused by ASR provide space for the deposition of ettringite. However, DEF can occur without ASR.

1.7 The DEF Problem

While the use of steam cured precast members may deliver initial returns in the form of speed of construction, historically, steam cured members have been plagued by reduced service life when compared to their normally cured cast-in-place counterparts. Research has ascribed differential thermal expansion as the cause of reduced strength in aged steam cured members and several techniques have been prescribed to stall the decline in strength [Soroka, 1978; Hanson, 1963; Pfeifer, 1981]. However, researchers have presented compelling evidence that deteriorating steam-cured members could also suffer

from delayed ettringite formation (DEF).

The frequent misdiagnosis of DEF as alkali-silica reaction (ASR) has compounded the confusion surrounding the role of DEF in the deterioration of concrete members. Some are quick to diagnose ASR since a standard test method to assess the potential for deleterious expansion of a concrete sample due to alkali-silica reaction of its aggregates is readily available [see ASTM C1293]. No standardized test is currently available for evaluating the potential for DEF. Consequently, the role of DEF in the decline of a concrete member may be overlooked.

Damage due to expansion coinciding with DEF may take years to manifest itself in the field. Thus, for practical reasons, an accelerated test method to assess the potential for expansion due to DEF in concrete samples and existing concrete members is sought by researchers. To that end, the accelerated test method proposed by Duggan et al [1987] is of interest, as it yields quantitative test data within days. Though the Duggan test does have its detractors, they cite the severity of its heating regime, the method by which cores are obtained, and question how representative the cores are of the concrete from which they are drilled. The Duggan test is essentially an accelerated expansion test. Since several factors including ASR contribute to expansion, the Duggan test alone cannot be used to prove or disprove the occurrence of DEF.

1.8 Proposed Approach for Evaluating DEF

As demonstrated by the work of Ramadan et al [2000] and Azzam et al [2002], a battery of tests can be used to evaluate the potential for DEF in a concrete mix under a variety of exposure conditions. The modified Duggan test as proposed by UMD/FHWA can be used to accelerate expansion in concrete samples. Under the modified test, expansion measurements are made per ASTM C490.

The time-dependence of the expansion is found by fitting the data to a kinetics model based on Kolmogorov-Avrami-Johnson-Mehl equation (KAJM). This provides a set of parameters to characterize the process which are more reliable than the expansion observed at a fixed time, as presently used in the ASTM and Duggan tests. This approach can also be used to isolate individual expansion mechanisms if they occur on different timescales. This analysis thus resolve contribution of DEF to the overall expansion results.

The presence of ettringite can be observed directly by a Scanning Electron Microscope (SEM), while Computed Tomography (CT) X-ray is useful in investigating the damage mechanism. Additionally, a quantitative analysis of the CT scans can be employed to determine the density of microcracks in the sample. This information, along with measured strain data, can be used to evaluate the status of the sample. For instance, a concrete sample that has undergone a strain due to expansion in excess of 0.3% is generally considered failed.

1.9 Problem Statement

The purpose of this research was to examine the influence of fine aggregates on delayed ettringite formation. The only factor that is allowed to vary is the type of fine aggregate which has an associated MDSHA expansion test rating. This is usually assumed to be a measure of ASR reactivity. Thus this research can establish the dependence of DEF on the fine aggregate expansion rating.

Also since ettringite is a hydrous phase of cement material, different exposure conditions including maximum exposure of the concrete sample to water were investigated.

1.9.1 Research Program Overview and Scope

The research project discussed included a comprehensive review of the literature and laboratory testing to study the influence of various fine aggregates on Delayed Ettringite Formation (DEF) in High Early Strength (Type III) Concrete. The scope of the research has been limited to three fine aggregates with a single unreactive coarse aggregate. The fine aggregates selected for the study vary in geographic place of origin, MDSHA expansion test rating, method of production, and petrographic makeup as detailed in Chapter 3: Fine Aggregate Selection and Sampling.

TABLE 1.1 – Major Portland Cement Constituents by Bogue Analysis

NAME	CHEMICAL FORMUAL	WEIGHT(%)
Tricalcium silicate	C_3S	52
Dicalcium silicate	C_2S	18
Tricalcium aluminate	C_3A	8
Tetracalcium aluminoferrite	C_4AF	8
Gypsum	CSH_2	-

Mass fractions representative of the specific cement sample used for the research project herein discussed as determined by Bogue analysis
X-ray fluorescence spectrometry (XRF). XRF analysis performed per ASTM C114-00. The XRF also included the oxide analysis presented in TABLE 2.1.

CHAPTER 2 - Test Materials Selection and Sampling

2.1 Portland Cement Selection and Sampling

The cement used for all batching was Portland cement Type III, which is commonly used to produce high early strength concrete. This type of cement was chosen because it is suspected of being particularly susceptible to DEF. In comparison to other cement types, Type III cement has a higher sulfate content, which would favor the crystallization of ettringite (Taylor, p.73). A chemical characterization of the cement used under this research project is made in Table 2.1.

To eliminate possible variation in the cement sample, all cement used originated from the same batch produced in Allentown, PA. Though the cement was purchased pre-packaged, all bags were thoroughly blended together in a drum mixer resulting in a uniform and consistent cement sample.

2.2 Fine Aggregate Selection and Sampling

The scope of this research project included only fine aggregates used in Maryland state highway projects. Three fine aggregates were selected from each possible MDSHA expansion test rating: low (0 – 0.09%), medium (0.10% – 0.19%), and high (0.20% - 0.29%). Fine aggregates with ratings above this range would usually not be acceptable in state highway projects. Aggregate Industries, Inc. currently distributes each of the fine aggregates selected for this study throughout the state of Maryland. A summary of aggregate test data and description follows in Table 2.2.

The location of the source of each fine aggregate is illustrated in Figure 2.1: Fine Aggregate Source Map. Two are produced in Maryland (Brandywine and Silver Hill) and one is produced in West Virginia (Millville). All applicable

ASTM test procedures were followed during the collection of the sands to ensure a sufficiently random sample (ASTM C-702, D-3665, and D-75).

2.2.1 Millville Fine Aggregate Selection and Sampling

Aggregate Industries, Inc. currently produces highly uniform and non-expansive sand in Millville, West Virginia. Railroad cars bring the sand to the company's Bladensburg plant where it is distributed throughout the state of Maryland[i].

The sand is milled from quarried limestone gravel. Since its ASR rating is very small (0.028%), this sand was considered to be a control sample.

2.2.2 Brandywine Fine Aggregate Selection and Sampling

Brandywine is produced from alluvial gravel collected from creeks and streambeds. By nature it is highly heterogeneous. According to the Maryland Geological Survey (Geologic Map of Maryland, 1968), this aggregate is composed of orange-brown siliceous gravel, locally limonite-cement in the Brandywine, and minor silt with red, white, or gray clay. The sand is also very coarse relative to the other two sands and it has a mild MDSHA expansiveness (0.14%).

The sand is part of an upper loam layer found in southern Maryland. The layer has a depth of up to fifty (50) feet from the surface.

2.2.3 Silver Hill Fine Aggregate Selection and Sampling

Silver Hill is a highly expansive natural sand. It is also very uniform in terms of color, morphology, and grading considering it was naturally produced. However, it contains a small amount of a deleterious substance (chalcedonic chert).

The sand is pale brown but weathers to white or at least pale gray. It is part of a fine-grained argillaceous sand layer found in southern Maryland with a depth of up to one hundred and fifty (150) feet from the surface.

2.3 Coarse Aggregate Selection and Sampling

To eliminate possible variables, only one coarse aggregate was used for all three concrete batches. The gravel is dolomitic limestone (see Figure 2.3) with a maximum diameter of one (1) inch. The gravel originates in Frederick, MD and has a dry rodded weight of 102.3 lb / ft with a specific gravity of 2.72. Its absorption is 3%. The physical characterization of the coarse aggregate, as published by the Aggregate Industries Labs, is presented in Table 2.3.

2.4 Selection of Potassium Carbonate as Admixture

The only admixture allowed under this research project was anhydrous granular reagent grade potassium carbonate (K_2CO_3). Its effect on the pore water chemistry is the same as naturally occurring potassium in unhydrated Portland cement. Potassium in cement primarily occurs as potassium sulfate (KSO_4). During hydration, the potassium sulfate exchanges ions with calcium and hydroxide to produce a potassium hydroxide solution and a calcium sulfate precipitate:

(1) $$K_2SO_4 + Ca^{2+} + 2OH^- \rightarrow 2K^+ + 2OH^- + CaSO_4$$

The potassium carbonate admixture hydrates as follows. The potassium carbonate exchanges ions with the calcium and hydroxide to produce a potassium hydroxide solution and a calcium carbonate precipitate:

(2) $$K_2CO_3 + Ca^{2+} + 2OH^- \rightarrow 2K^+ + 2OH^- + CaCO_3$$

. Since the number of hydroxide moles on both sides of equation 1 and 2 remain constant, neither reaction affects the pH of the mix. The advantage of adding potassium carbonate rather than potassium sulfate is that the former does not increase the sulfate content, which also favors DEF.

The potassium carbonate was added directly to the mix water to achieve a target potassium level of 1.50% by weight of cement or 1.41% by weight of the mix water. The target potassium level included the added potassium plus the natural potassium in the cement, in this case potassium sulfate.

FIGURE 2.1 - Fine Aggregate Source Map

"X" marks the location of each of the three fine aggregates selected for this research: Millville (in West Virginia), Crain Highway (Silver Hill, Maryland), and ELG (Brandywine, Maryland). Millville is transported on the rail link shown to its distribution at the Bladensburg plant.

FIGURE 2.2 – Fine Aggregate Selection

Sample diversity was a key criterion in the fine aggregate selection process. The three sands chosen differ in their place of origin, method of production, ASR expansiveness, particle size distribution (Grading), and petrographic / morphologic characteristics. Millville is a dark gray nonexpansive manufactured sand from quarried limestone. Brandywine is a light brown mildly expansive manufacture sand from natural gravel. Silver Hill is a tan highly expansive natural, silicate sand.

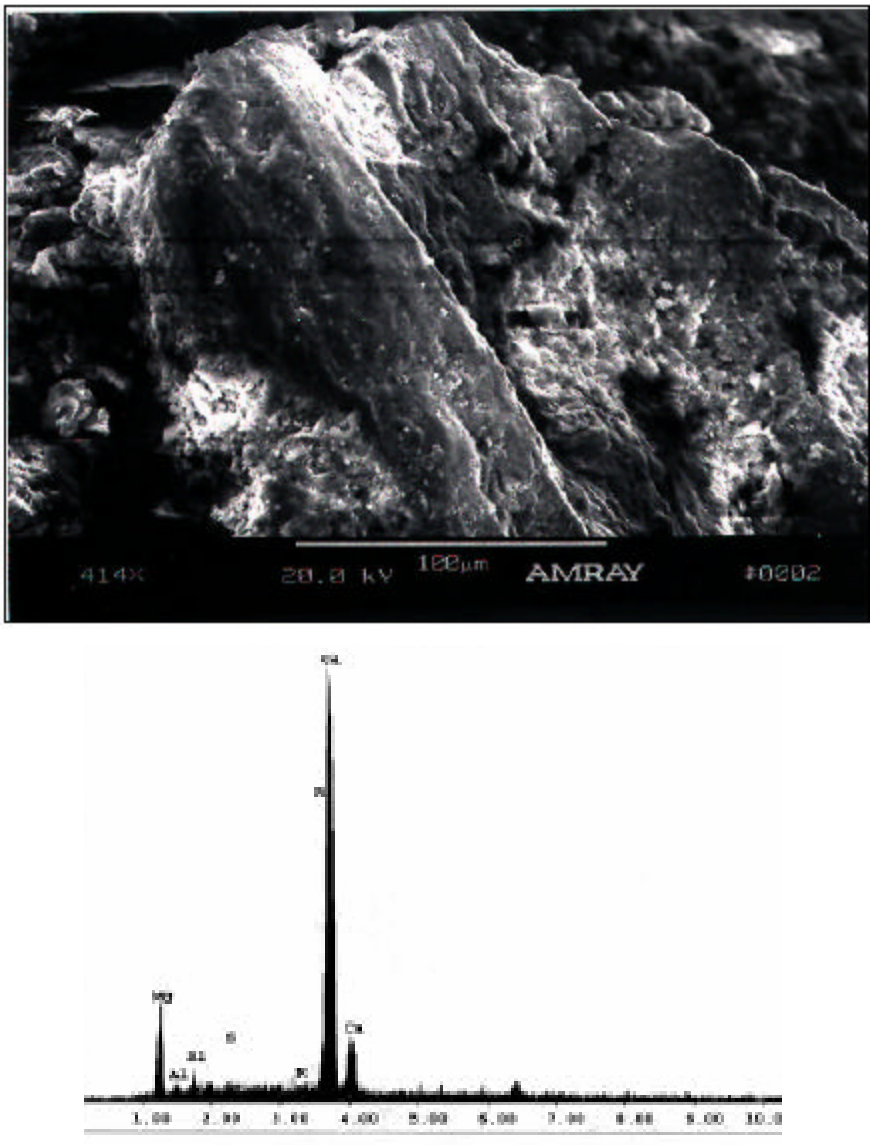

FIGURE 2.3 – EDAX Identification of Coarse Aggregate

The photograph above and accompanying EDAX spectrum is of a piece of coarse aggregate. The magnesium peak is well defined. Especially for an element that is not very fluorescent (when compared to elements like calcium for instance). The presence of magnesium in the spectrum provides strong evidence for identifying the coarse aggregate as dolomitic limestone.

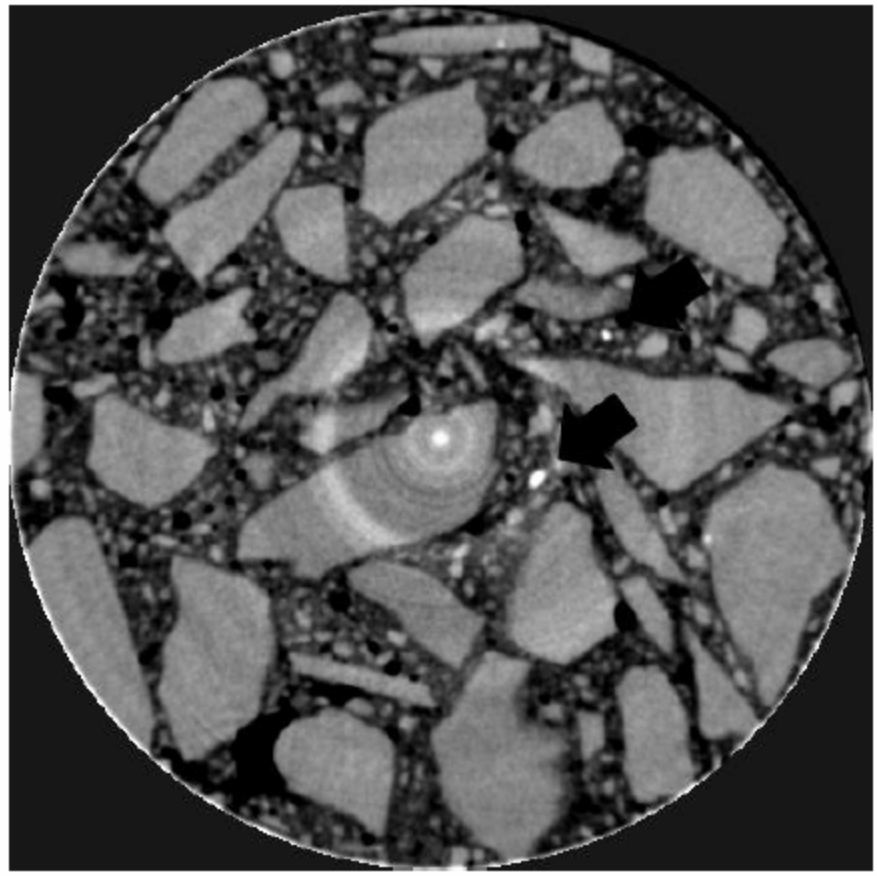

FIGURE 2.4 – Iron Ore Spotted in X-ray

Bright areas were commonly spotted in X-ray cross sections of concrete cylinders. White areas in the image indicate high density. These are most likely fragments of iron ore from the coarse aggregate.

TABLE 2.1 –Cement Oxide Analysis

Analyze	Weight %
SiO_2	20.01
Al_2O_3	4.95
Fe_2O_3	2.74
CaO	62.08
MgO	2.57
SO_3	4.13
Na_2O	0.40
K_2O	0.92
TiO_2	0.21
P_2O_3	0.11
Mn_2O_3	0.05
SrO	0.22
Cr_2O_3	0.01
ZnO	0.03
L.O.I. (950°C)	1.59
Total	100.00
Alkalics as Na_2O	1.01

X-ray Fluorescence (XRF) spectrometry was used to determine the mass fractions of the cement's constituents and oxides. Of special interests are the elevated level of sulfate (SO_3) and the level of potassium (K_2O). In general, high levels of sulfate is favorable to DEF in concrete. The reported potassium level was used to correctly determine the amount of potassium carbonate (K_2CO_3) needed in the mix water to achieve the target potassium level of 1.50% by weight of cement.

TABLE 2.2 – Physical Characterization of Fine Aggregates

NAME	MILLVILLE	BRANDYWINE	SILVER HILL
ORIGIN	MILLVILLE QUARRY, INC.	E.L. GARDENER, INC.	SILVER HILL MATERIALS
CERTIFICATION DATE	25-Apr-02	20-Feb-02	31-May-02
METHOD OF PRODUCTION	MANU. SAND FROM MANU. GRAVEL	MANU. SAND FROM NATURAL GRAVEL	NATURAL SAND
SIEVE ANALYSIS			
3/8"	100%	97%	100%
#4	97%	6%	97%
#8	94%	2%	83%
#30	55%	0.90%	47%
#50	23%	0.75%	22%
#200	1.50%	0.30%	1.20%
PHYSICAL PROPERTIES			
ABSORPTION (ASTM C-128)	0.66%	1.20%	0.90%
BULK SP GRAVITY (ASTM C-128)	2.826	2.59	2.61
SOUNDNESS (ASTM C-88) MAGNESIUM SULFATE	4.259% LOSS	2.73% LOSS	1.3% LOSS
ASR	0.028%	0.14%	0.28%
PETROGRAPHIC EXAMINATION			
	87.1% DOLOMITIC LIMESTONE 7.3% LIMESTONE	UNKNOWN VARIES	85.3% QUARTZ 8.9% QUARTZOSE SANDSTONE 1.5%CHALCEDONIC CHERT

All test data provided courtesy of Aggregate Industries Labs. Data as reported in current letter of certification.

TABLE 2.3 – Physical Characterization of Coarse Aggregates

RGI Fredrick Quarry ASTM #57 Stone Physical Analysis		
Rock Type:	Carbonate Calcitic Limestone	
Color:	Light Gray	
Average Gradion	**Dry Analysis**	**Wet Analysis**
ASTM C136	**% Passing**	**% Passing**
1 (in.)	100	100
3/4 (in.)	97.3	92.7
1/2 (in.)	48.3	44.1
3/8 (in.)	26.0	18.1
#4	15.1	3.0
#8	1.9	1.1
Pan	1.1	0.1

	Bulk	SSD
Specific Gravity (AASHTO T85)	2.712	2.722
Absorption (AASHTO T85)	0.40%	—
200 Wash (ASTM C117)	0.80%	
Polish Value (MSMT 411)	7	—
British Pendulum Number (ASTM D411)	26	—
Alkali Silica Reactivity (MSMT 212/ ASTM C1260)	0.09% Expansion	—
L.A. Abrasion (AASHTO T96/ ASTM C131	26% Wear	—
Sodium Sulfate Soundness (AASHTO T104)	0.1% Loss	—
Unit Weight, Dry Rodded (AASHTO T19)	99#/CF	—
MOHs Hardness	4	—
Sand Equivalency (AASHTO T176)	94%	—
Fractured Faces (PMT 621)	100%	—

All test data provided courtesy of Aggregate Industries Labs. Data as reported in current letter of certification. Only Fredrick, MD coarse aggregate was used under this research project.

CHAPTER 3 – Concrete Sample Preparation and Treatment

3.1 Concrete Mix Design

All concrete mix proportioning and preparation were done according to ASTM C 192M – 95 and current Portland Cement Association (PCA) guidelines. The absolute volume method was used to proportion the concrete mixes. All concrete batches had a water-to-cement ratio of 0.50. The target twenty-eight (28) day compressive strength for all batches was 5,000 psi. Final batch size data and mix cycle design are shown in Tables 3.1 and 3.2.

The fine aggregate type was the only variable among the batches. Since the moisture content, unit weight, and adsorption of the fine aggregate impact proper mix proportioning, the proportions of each batch varied. The final proportions of Batches #1 thru #3 are recorded in Tables 3.3 thru 3.5. All batches were a total of two (2) cubic feet in volume. Adjustments were also made for the moisture content and absorption of the gravel, which were 0.10% and 0.50% respectively.

3.2 Mix Cycle Design

All concrete test specimens were mixed in accordance with ASTM C 192M – 95. A six (6) cubic yard drum mixer with a rotation rate of twenty-five (25) rpm was used for all batches. The cycle began with just the mixing of the pre-loaded sand and gravel. Then water and cement were added separately at equal intervals. Mixing was concluded after a brief pause. The cycle covered an elapsed time of nine (9) minutes.

The expected set time of the concrete was the major constraint in designing the mix cycle. With a relatively high potassium level (1.50% by weight of cement) and low water-to-cement ratio (0.50), the mix cycle duration had to be

limited to ensure adequate workability and compaction in the sample molds. The mixing of all batches proceeded as recorded in Table 3.2.

3.3 Batch Size Requirements

A minimum of five (5) 3”x3”x10” prisms and nine (9) 4”x8” cylinders per set are required to measure expansion and compressive strength with acceptable error. Additional samples were cast for the Scanning Electron Microscope (SEM) and X-ray analysis.

Only Batch #3, made with the low ASR sand, included all exposure conditions (see Figure 3.6). Batch #1 and Batch #2 included only the wet and submerged conditions. Final batch size and information is summarized in Table 3.1.

Smaller (1 ft^3) supplemental batches of Batch #1 thru Batch #3 were cast to provide additional cylinders for X-ray Computed Tomography (CT) and prisms for Scanning Electron Microscope (SEM) work. Refer to Chapter 4: Tests and Test Frequency for a complete discussion of the application of CT and SEM in this research program.

3.4 Sample Preparation Sequence

All samples where prepared and cured in accord with ASTM C 192M – 95. Concrete samples were cured and heat-treated before being stored in environmental chambers. The sample preparation sequence was sixteen (16) days in duration (see Figure 3.1).

3.4.1 Mold Size

Concrete prisms were cast in reusable steel molds with a single compartment measuring 3” x 3” x 11.25”. The molds had inserts for steel gauge studs. Studs were installed for length change measurements per ASTM C490-86. The prism models were lightly coated with a form release agent before each use

in compliance with ASTM C470. Ramadan et al (2000)[ii] prescribed the prism size used.

The cylinder molds were 4" X 8" PVC containers. This mold size complied with ASTM C192 by having a cross sectional dimension (i.e. diameter) at least three (3) times larger then the nominal size of the coarse aggregate which in this case was one (1) inch. Both mold types were able to hold their standard dimensions within acceptable tolerances under test conditions and were watertight per ASTM C470.

3.4.2 Casting

All concrete batches made under this research program were proportioned with a low water-to-cement ratio (0.5) and high potassium content (1.50% by weight of cement), which produced a very dry mix with low workability and reduced set time. These factors made adequate consolidation in the molds a challenge.

Since the slump was less than one (1) inch, a table vibrator[iii] was used to consolidate the concrete in the molds per ASTM C192. The table vibrator used had a surface area of approximately four (4) square feet and accommodated up to four (4) cylinders and two (2) prisms at one time. The molds were held down as close to the center of the tabletop as possible to insure maximum energy transfer from the vibrating surface to the molds.

Casting began by placing the empty molds on the vibrating table, which was set to maximum (approximately 60 Hz). The molds were then filled incrementally with two equal layers of concrete. The molds were left on the vibrating surface for up to ten (10) seconds. This technique yielded excellent consolidation despite the difficult workability issues.

The molds were stripped after 24 ± 8 hours per ASTM C192. Very little honeycombing, a symptom of under consolidation was discovered in the freshly

stripped samples (see Figure 3.3). No segregation of the coarse aggregate, as a result of over consolidation, was found.

3.4.3 High Temperature Curing

All high temperature samples were cured almost immediately after casting (usually within 1 hour). The goal was to simulate commercial steam curing using the conventional ovens available in the lab. The samples were placed in the oven with pans or bowls full of water. The oven was then preset to 85° C and left to run for four (4) hours.

3.4.4 Low temperature Curing

One day after casting, the samples were submerged in limewater at room temperature (21° C) and allowed to continue curing for seven (7) days. The lime or calcium hydroxide [$Ca(OH)_2$] prevents leaching between samples and is a requirement for water storage per ASTM C192 .

The samples where then heat-treated using the Duggan Cycle. After sitting at room temperature (about 24° C) for two (2) days in a dry container, the samples were finally placed in controlled moisture environments for long-term storage. The sample preparation sequence proceeded as recorded in Figure 3.1.

3.4.5 Exposure / Storage Conditions

Under this research program, samples were stored in one of three exposure conditions (see Figure 3.2). Details of each exposure condition are summarized in Table 2.4. It is here noted that “SUBMERGED” means storage in limewater. ASTM C192M-95 requires concrete samples to be stored in limewater as opposed to a plain water bath to stimulate pH conditions in actual concrete.

TABLE 3.1 – Final Batch Size Data

	BATCH #1	BATCH #2	BATCH #3
Fine Aggregate	Silver Hill	Millville	Brandywine
Date Cast	8/15/2002	8/22/2002	8/28 - 8/29/2002
Exposure Conditions	WET/SAT.	WET/SAT./SUB.	WET/SAT.
Total Cylinders	22*	32*	20
Total Prisms	27*	30	20
	BATCH #1b	**BATCH #2b**	**BATCH #3B**
Cast Date	5/27/2003		
Total Cylinders	1	1	1
Total Prisms	4	4	4

The final sizes of the first three batches are recorded above. The supplemental batches (Batches #1b - #3b) were cast with equal numbers of prisms and cylinders. Batch size requirements were set to provide a minimum number of samples needed to insure acceptable statistical precision for the expansion and compression tests. The batch size requirement was ten (10) prisms and cylinders per exposure condition. Therefore, with two exposure conditions, batches #1 and #3 were required to have a minimum of twenty (20) prisms and cylinders each. Batch #3 was required to have a minimum of thirty (30) prisms and cylinders since it included three exposure conditions. The prisms of the supplementary batches were evenly distributed among the exposure conditions. Each cylinder for batches #1b - #3b was kept dry.

* Extra samples were kept under dry conditions and were not used during this research.

TABLE 3.2 – Mix Cycle Design

MIX CYCLE DESIGN		
ELAPSED TIME	**TIME INTERVAL**	**DESCRIPTION**
0 sec.	30 sec.	MIX SAND & GRAVEL
30 sec.	30 sec.	ADD WATER
1 min.	180 sec.	ADD CEMENT
4 min.	180 sec.	INITIAL MIX
7 min.	120 sec.	PAUSE
9 min.	--	FINAL MIX

The expected set time of the concrete was the major constraint in designing the mix cycle. The mix cycle duration had to be limited to ensure adequate workability and compaction in the sample molds.

TABLE 3.3 - Concrete Mix Proportioning of Batch #1 (Silver Hill)

BATCH #1		AUG. 15, 2002	
GIVEN DATA		UNIT WEIGHTS	
FINE AGG:	SILVER HILL	TOTAL WATER:	300 lb/yd
28-DAY STRENGTH:	5,000 psi	CEMENT:	600 lb/yd
GRAVEL SIZE:	1 in.	GRAVEL:	1890 lb/yd
GRAVEL WEIGHT:	100 pcf	SAND:	1335 lb/yd
W/C:	0.50	CONCRETE:	4125 lb/yd
AIR-CONTENT:	~1.5%		
MATERIAL		ADJUSTMENT	TOTALS
GRAVEL:		1891.8 lb/yd	140.1 lb
SAND:		1362.1 lb/yd	100.9 lb
MIX WATER:		286 lb/yd	21.1 lb
CEMENT:		-	44.4 lb
POTASSIUM:		-	0.299 lb

The adjustments made were for the moisture content and absorption of the sand and gravel, which were 1.99% and 0.1% respectively.

TABLE 3.4 - Concrete Mix Proportioning of Batch #2 (Millville)

BATCH #2		AUG. 22, 2002	
GIVEN DATA		UNIT WEIGHTS	
FINE AGG:	MILLVILLE	TOTAL WATER:	300 lb/yd
28-DAY STRENGTH:	5,000 psi	CEMENT:	600 lb/yd
GRAVEL SIZE:	1 in.	GRAVEL:	1890 lb/yd
GRAVEL WEIGHT:	100 pcf	SAND:	1428 lb/yd
W/C:	0.50	CONCRETE:	4218 lb/yd
AIR-CONTENT:	~1.5%		
MATERIAL		ADJUSTMENT	TOTALS
GRAVEL:		1914.3 lb/yd	137.4 lb
SAND:		1294.2 lb/yd	102.3 lb
MIX WATER:		256.1 lb/yd	18.9 lb
CEMENT:		-	44.4 lb
POTASSIUM:		-	0.299 lb

The adjustments made were for the moisture content and absorption of the sand and gravel, which were 2.10% and 0.1% respectively.

TABLE 3.5 - Concrete Mix Proportioning of Batch #3 (Brandywine)

BATCH #2		AUG. 22, 2002	
GIVEN DATA		UNIT WEIGHTS	
FINE AGG:	MILLVILLE	TOTAL WATER:	300 lb/yd
28-DAY STRENGTH:	5,000 psi	CEMENT:	600 lb/yd
GRAVEL SIZE:	1 in.	GRAVEL:	1890 lb/yd
GRAVEL WEIGHT:	100 pcf	SAND:	1428 lb/yd
W/C:	0.50	CONCRETE:	4218 lb/yd
AIR-CONTENT:	~1.5%		
MATERIAL		ADJUSTMENT	TOTALS
GRAVEL:		1914.3 lb/yd	137.4 lb
SAND:		1294.2 lb/yd	102.3 lb
MIX WATER:		256.1 lb/yd	18.9 lb
CEMENT:		-	44.4 lb
POTASSIUM:		-	0.299 lb

The adjustments made were for the moisture content and absorption of the sand and gravel, which were 1.86% and 0.1% respectively.

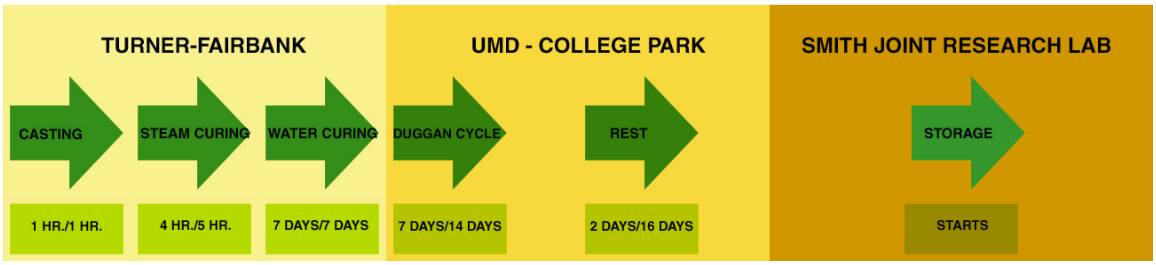

FIGURE 3.1: Sample Preparation Sequence

The preparation of the prisms and cylinders used for this research involved a six (6) step process that took sixteen (16) days to complete. In the process, the samples passed through two different labs on the way towards long-term storage at the Smith Joint Research Lab.

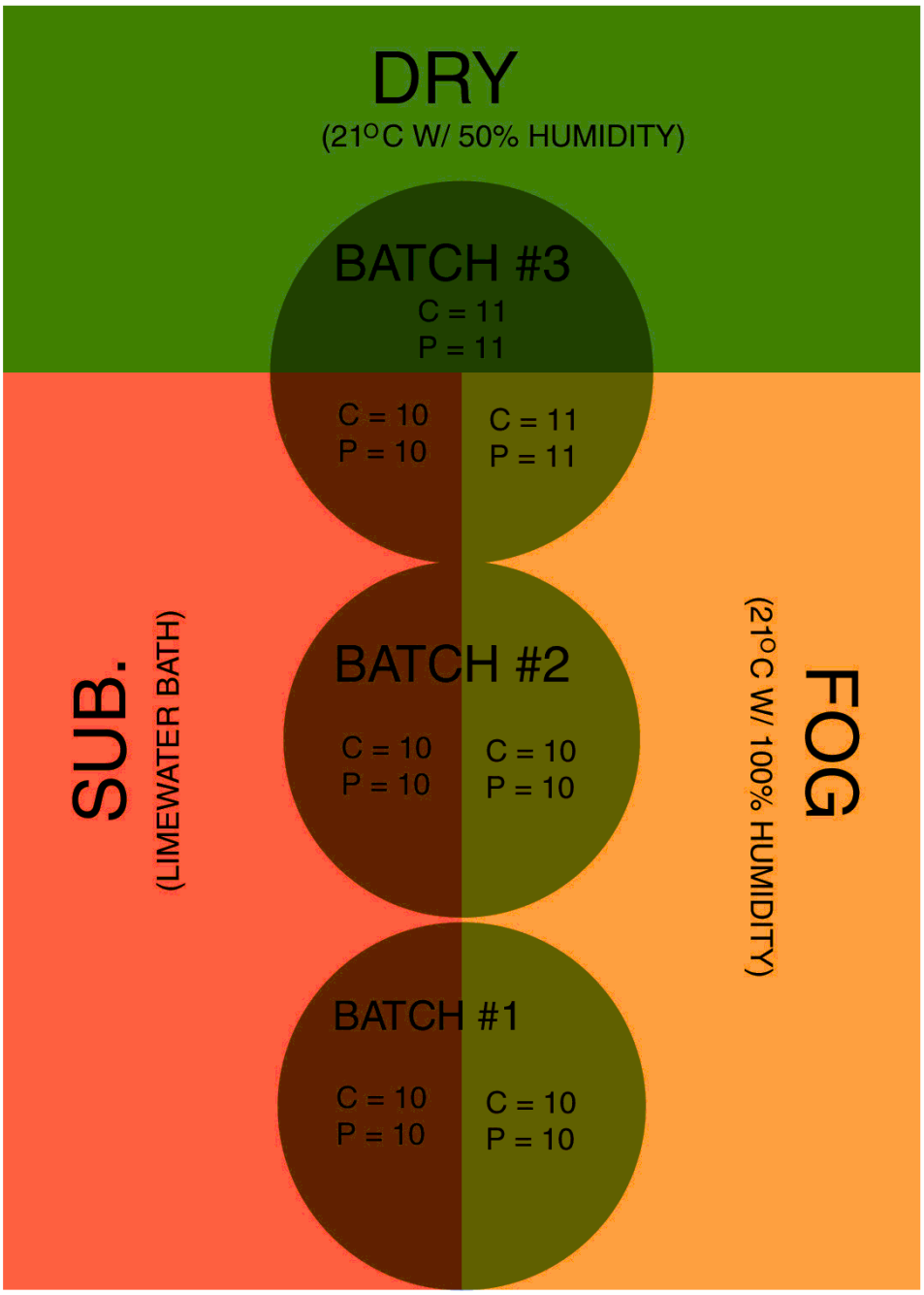

FIGURE 3.2 – Concrete Sample Distribution

Samples of Batches #1 and #2 were split evenly between the wet and saturated exposure conditions. Batch #3, made from the non-expansive fine aggregate, Millville, was divided evenly among all three exposure conditions.

CHAPTER 4 - Tests and Test Frequency

4.1 Test Locations

The expertise of the staff and resources of three outstanding research centers was used in preparation, treatment, and testing of all concrete specimens produced under this research program. A detailed discussion of the research activities conducted at each center follows.

4.1.1 Turner-Fairbank Highway Research Center (TFHRC)

Turner-Fairbank Federal Highway Research Center (TFHRC) is a campus of premier research facilities located in McLean, Virginia. The center is Federally owned and operated and conducts progressive research in over one hundred (100) disciplines. TFHRC serves the Federal Highway Administration (FHWA) and the world highway community at large by developing and testing state–of–the–art highway technologies. The staff of TFHRC's Concrete Laboratories specializes in the development and evaluation of test methods in concrete materials research. They also have experience in concrete forensics and the handling of new concrete products. With the exception of three small supplementary batches, all major batching and mixing of concrete specimens, including steam curing, was conducted in the Plastic Concrete laboratory at TFHRC between June and August of 2002.

The lab is equipped with drum and pan mixers, ovens, and environmental chambers. The concrete samples where produced under tightly controlled laboratory conditions and under the supervision of trained lab technicians adept in all applicable ASTM test procedures.

A nondestructive analysis of concrete cylinders was conducted using the equipment housed in the NDEVC labs. A detailed description of how Computed Tomography (CT) X-ray and Radiography was applied under this research program follows in Section 4.5.

Destructive tests on concrete prisms using a Scanning Electron Microscope (SEM) were also conducted in a lab at TFHRC. A complete discussion of how Scanning Electron Microscope (SEM) Spectrometry with EDAX® Software was applied under this research program follows in Section 4.7.

4.1.2 Alfred H. Smith Joint Research Laboratory

Until recently, the Alfred H. Smith Joint Research Laboratory was jointly owned and operated by the National Aggregates Association (NAA) and the National Ready Mixed Concrete Association (NRMCA). The laboratory is located near the University of Maryland in College Park. Research at the Smith Joint Research Laboratory is conducted in support of concrete industry organizations including ACI and ASTM along with state and federal transportation agencies.

The laboratory is equipped with two large environmental chambers, one constant temperature fog room and one constant temperature dry room, in which all test samples used under this research program were stored. All compression and expansion tests, as discussed in detail in Sections 4.4 and 4.5 respectively, were conducted at Smith Joint Research Laboratory.

4.1.3 Structural Engineering Laboratory at University of Maryland – College Park

The heating cycle prescribed by the Duggan Test was conducted in the Structural Engineering Laboratory at the University of Maryland in College Park. The oven used to heat treat the samples is equipped with a compressor and is capable of refrigeration in addition to heating. The oven had a programmable digital controller and operated within a range of -20° C to 100° C. It was selected because of its ability to rapidly heat the samples[15] and hold a pre-programmed temperature within a tenth of a degree Celsius (± 0.05° C).

4.2 X-ray Fluorescence Spectrometry (XRF)

Oxide analysis by X-ray Fluorescence Spectrometry (XRF) meets the precision and accuracy requirements for rapid test methods per ASTM – C114-00. As such, the test is commonly used to identify the constituents of concrete and mortar materials including cement, fly ash, slag, and aggregates.

An XRF analysis was performed by a specialty firm on a representative sample of the overall blended cement sample used under this research program. The analysis revealed a 0.92% potassium level by weight of cement. The potassium occurs naturally in the cement as potassium sulfate minerals. This data was used to calculate the necessary amount of potassium carbonate needed in the mix water to achieve the target constant potassium level (1.50% by weight of cement) of the concrete batches.

4.3 Duggan Test

Under this research project, the Duggan heat cycle was used to initiate cracking in the specimens. The test measures length change of concrete cores that have been heat-treated using a prescribed heating regime. The heating cycle is intended to induce hairline cracks in the samples through differential thermal stresses.

Though the test collects expansion data, the Duggan test may be more than merely an accelerated expansion test. Research has confirmed that the amount of expansion occurring within the first twenty (20) days of the test directly correlates to the amount of ettringite that forms during that period [Attiogbe and Well, 1990].

4.3.1 Duggan Sample Preparation Method

The specimens used in this research differ from the core samples that are recommended for use in the Duggan test. Duggan suggested the use of cores one (1) inch in diameter and two (2) inches in length with parallel and smooth ends.

The concrete cores can be drilled from existing structures or laboratory samples as long as they are appropriately sized.

Before heat treatment, the cores are soaked in water at room temperature (21° C). Then their initial lengths are recorded.

4.3.2 Modified Duggan Sample Preparation Method

The use of cores allows for sampling from a general source of concrete that may be of interest including existing structures. However, when laboratory specimens are used, this method of obtaining test samples is unduly arduous. Therefore, under this research program, a modified Duggan Sample Preparation method, proposed by UMD/FHWA, was used.

The modified sampling technique uses prisms (3" x 3" x 11") cast from concrete mixed in a laboratory instead of the cores Duggan suggested. The prisms are made with end steel inserts for linear length change measurements following ASTM C192-88 and ASTM C1293 (see Figure 4.1). Before heat treatment, the initial lengths of the prisms are recorded.

4.3.3 Duggan Test Heating Cycle

The Duggan test heating cycle is an eight (8) day heating regimen with prescribed intervals of heating and cooling at specific temperatures and duration. The heating temperature is eighty-two (82) degrees Celsius and the cooling temperature is twenty-one (21) degrees Celsius. One complete cycle includes both a period of heating and cooling.

The first two cycles are identical and include one day of heating followed by one day of cooling. The samples are cooled in a limewater bath. The third and final cycle involves three days of heating followed by a day of cooling. Refer to Figures 4.2 and 4.3 for a graphical representation of the Duggan test heating cycle.

It is here noted that water-cooling can have its drawbacks especially when dealing with a large temperature gradient, in this case from 82° C to 21° C. Water is an excellent conductor of heat and has the potential of rapidly cooling concrete samples, particularly those of the size used in this experiment, thus causing excessively large cracks in the sample. To avoid this potential problem, the samples where allowed to cool in air for no more than one (1) hour before placement in the water bath.

4.4 Compression Test

Compression tests per ASTM C39-96 were conducted on (4" x 8") cylinders to determine their uniaxial compressive strength. Approximately one third (1 / 3) of the total cylinders made for this research program were used for twenty-eight (28 ± 1) day compression tests. The remaining cylinders were used for long-term compression tests, approximately two hundred and fifty (250) days. To ensure acceptable statistical precision, a minimum of three cylinders from each sample type was required for the compression tests.

With a few exceptions, the compression specimens were tested at a load rate of 25,000 lb / min. Some of the submerged cylinders had suffered an extreme strain due to expansion by the time of the second compression test and were consequently labeled as "failed". These samples where tested at a much lower loading rate of 2,500 lb / min.

4.5 Expansion Test

The standard test method for length change measurements, ASTM C490-86, provides for the equipment used to prepare the sample, in this case (3"x 3"x11.25") steel prism molds, and the apparatus used to make the length change measurements.

Under this research program, expansion / contraction measurements were made using a length comparator with a digital display accurate to ± 0.0005

inches. Since length is dependent on ambient room temperature, the length change measurements were made relative to a standard invar bar; though the length change readings were made in a constant temperature dry room.

The length change measurements were made at least once per week at three (3) to five (5) day intervals. To ensure acceptable statistical precision, a minimum of three prisms from each sample type was needed for the expansion tests. On average, ten (10) prisms were used from each sample type for length change measurements made during this experiment.

4.6 Computed Tomography (CT) X-ray and Radiography

Computed Tomography (CT) X-ray and Radiography was used to study internal cracking patterns of pre-designated concrete cylinders. The cylinders prepared for CT scanning contained lead rod inserts. The rods appeared as white circles on the X-ray cross-sections and provided orientation during a comparison of the X-ray images. Two (2) cylinders from each of the seven (7) sample types were used for CT scanning. The initial CT scan was made prior to heat treatment by the Duggan cycle. Subsequent CT scans of the cylinders were made after heat treatment was complete. Multiple scans of the same cylinder were compared as an attempt to track internal crack propagation. The scanning parameters of the CT X-ray are discussed presently.

The X-ray source was a continuous 2-milli ampere (mA) current with a 400 Kilo-electron (keV) voltage. Two-dimensional slices were generated using an array of 512-channel cadmium tungstate (CdWO4) array using scintillators coupled to Si photodiodes. Each scintillator had a thickness of 0.25 mm and a length and width of 5 mm.

Each X-ray image consisted of 512 x 512 pixels and represented a 0.8 mm thick slice of the cylinder. Imaging software was used to combine the X-ray images to produce a three dimensional image of the entire cylinder.

4.7 Scanning Electron Microscope (SEM) Spectrometry with EDAX® Accessory

Under this research project, a Scanning Electron Microscope (SEM) with an EDAX energy-dispersive analyzer was used to investigate the mechanism of concrete failure. SEM technology has been successfully applied to the investigation of concrete in this way for over twenty (20) years (Marusin, 1995).

The SEM can be used to study the elemental composition and morphology of a concrete sample. This is accomplished by directing an accelerated electron beam with a voltage of ten (10) to twenty (20) keV at the sample. Interaction between the beam and the sample surface causes the sample to fluoresce. The energy-dispersive analyzer registers three signal types: secondary electrons, backscattered electrons, and X-ray. The analyzer tracks the atomic number of each backscattered electron it receives which leads to the elemental identity of the particles from which the electrons came. The EDAX® software adjusts for atomic number, absorption, and fluorescence (ZAF) to produce a semi-quantitative analysis showing the fractional weights of each element identified on the sample surface. The secondary electrons are used to generate an image of the surface.

4.7.1 SEM Sampling Technique

The usefulness of SEM studies depends mainly on the sample selection and preparation technique employed by the researcher. It takes an in-depth knowledge of the material being investigated, skill, and experience to select and prepare representative specimens. In 1995 Stella L. Marusin published a comprehensive comparison of SEM test results using various sample preparation techniques including Thin Sections (TS), Epoxy-impregnated Thin Sections (FTS), Epoxy-impregnated Sawn Polished Surfaces (ESPS), Sawn Polished Surfaces (SPS), Sawn Unpolished Surfaces (SUS), and finally Fractured Surfaces (FS). Marusin concluded that fractured surfaces where best for investigations into DEF and perhaps failure mechanisms in general.

However, fracturing specimens from a larger piece of concrete, usually by means of blows from a hammer, 'disturbs' the sample by introducing cracks that were not present before sampling began. Therefore, a general investigation of the distress in a concrete sample, which considers internal crack patterns as well as failure mechanism, may include several sampling techniques. While fractured surfaces are ideal for spotting ettringite crystals at the cement paste – aggregate interface, sawn surfaces, both polished and unpolished, can be used to examine internal crack patterns. Under this research project, internal crack patterns were investigated using Computed Tomography (CT) X-ray and radiography analysis.

4.7.2 Preparation of Fracture Surfaces for SEM Spectrometry

Specimens are broken from 3" x 3" x 11" concrete prism by means of hammer blows. To collect the fractured surfaces, the prisms where sliced into three (3) equal segments each approximately four (4) inches in thickness (Figure 4.4). The slices where placed in a plastic bag and broken using a hammer to expose fresh surfaces.

Fragments were then sampled from the bag and sorted into groups of "internal" or "external" chips. External fragments were defined as a fragment with a surface in common with the outside surface of the prism. The outside surface made the external fragments readily identifiable. Generally, ideal fragments were between 2-10 mm in size, flat, and included at least one cement paste-aggregate interface or water void.

The chips were mounted with carbon paint to half-inch diameter carbon stubs and dried at 55° C in a vacuum oven (Figure 4.5). The samples were then coated with a film of carbon approximately 100 Angstroms thick (1 Angstrom = 10^{-6} cm) to insure electrical conductivity and thus prevent charging effects in the microscope (Figure 4.6).

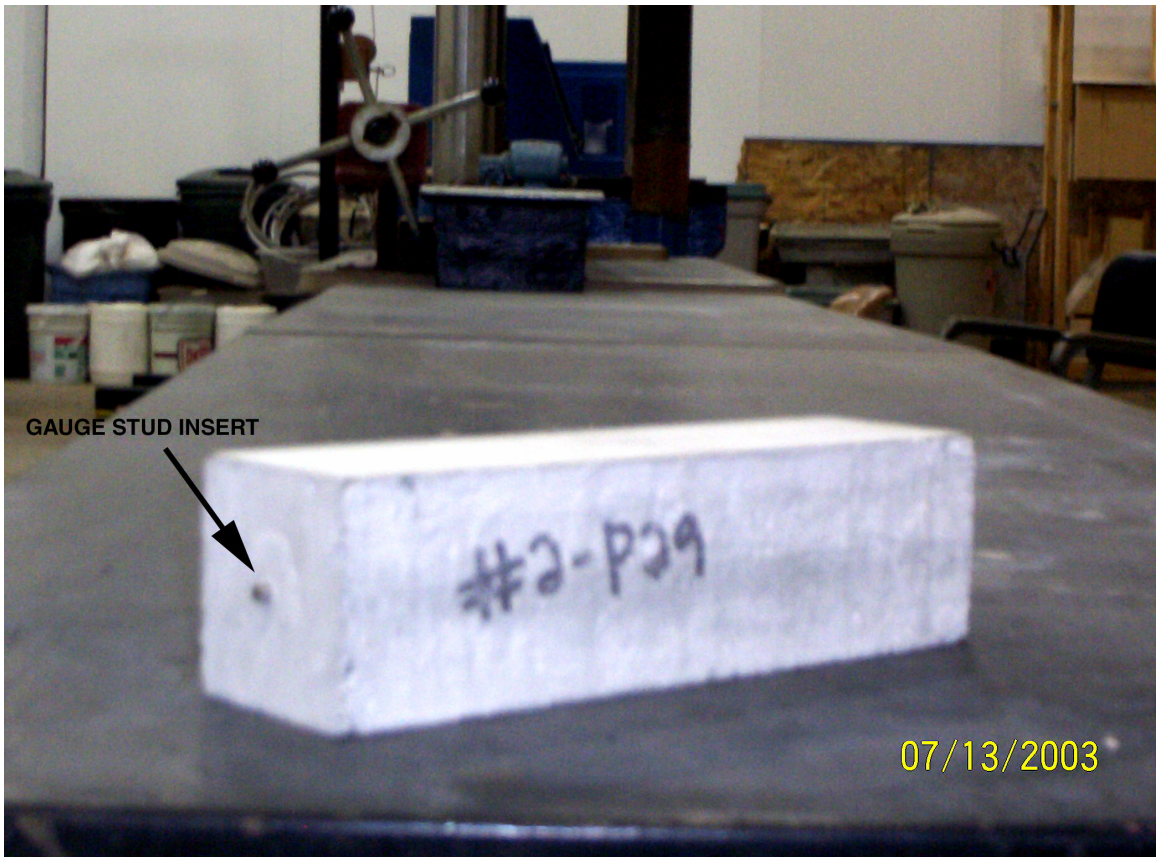

FIGURE 4.1 – Modified Duggan Sample Preparation Method

The modified sampling technique uses prisms (3” x 3” x 11”) cast with steel inserts at both ends for linear length change measurements following ASTM C192-88 and ASTM C1293. Before heat treatment, the initial lengths of the prisms are recorded.

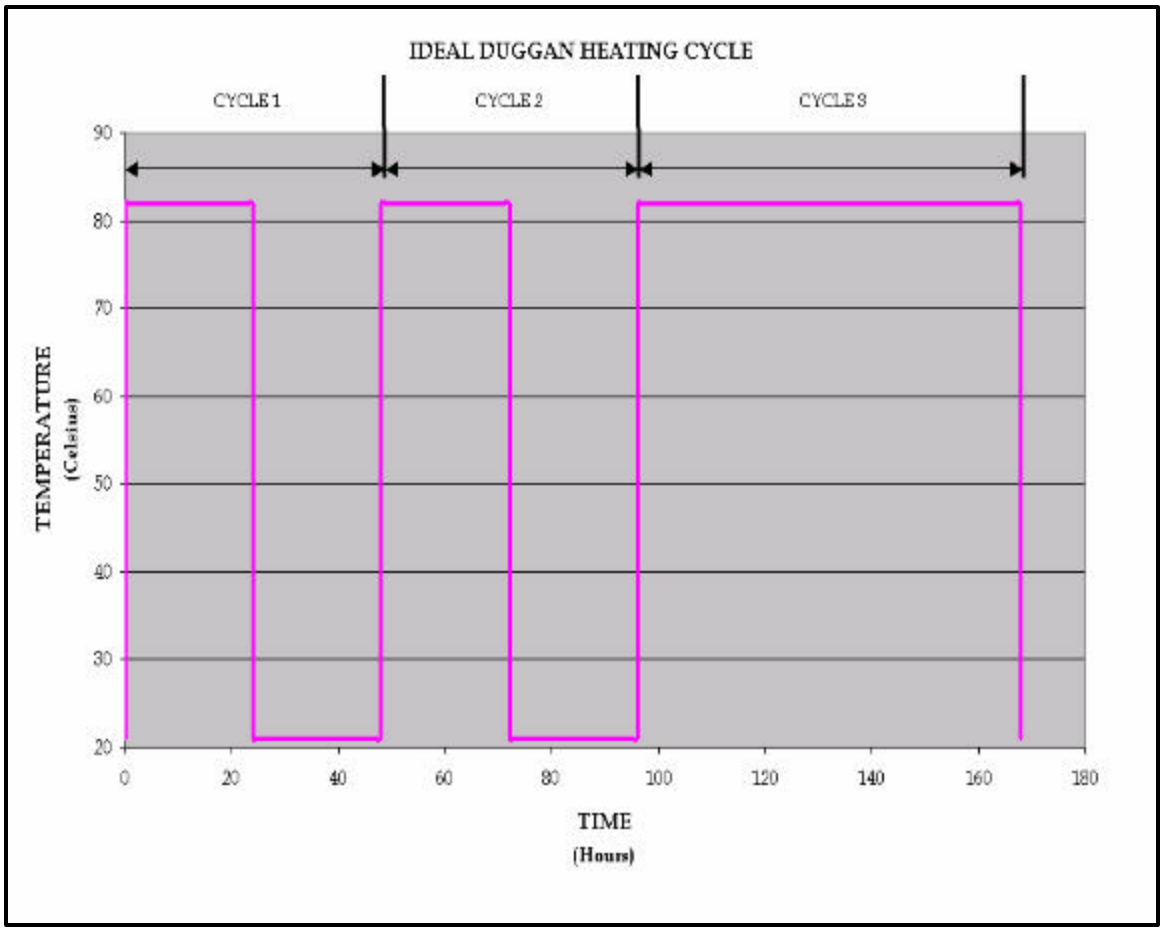

FIGURE 4.2 – Ideal Duggan Heating Cycle

The Duggan cycle is an eight (8) day heating regimen with two prescribed temperatures, 82° C being the maximum and 21° C the minimum. No time is allowed for 'heating' or 'cooling' between the two extremes, thus the ideal Duggan cycle graphed above. One complete cycle includes both temperatures. The first two cycles are identical with one (1) day at each temperature and the third cycle being the longest with an extended period of three days at the maximum temperature. The cycle prescribes water-cooling (i.e. storage at minimum temperature), while heating can be done in a conventional oven.

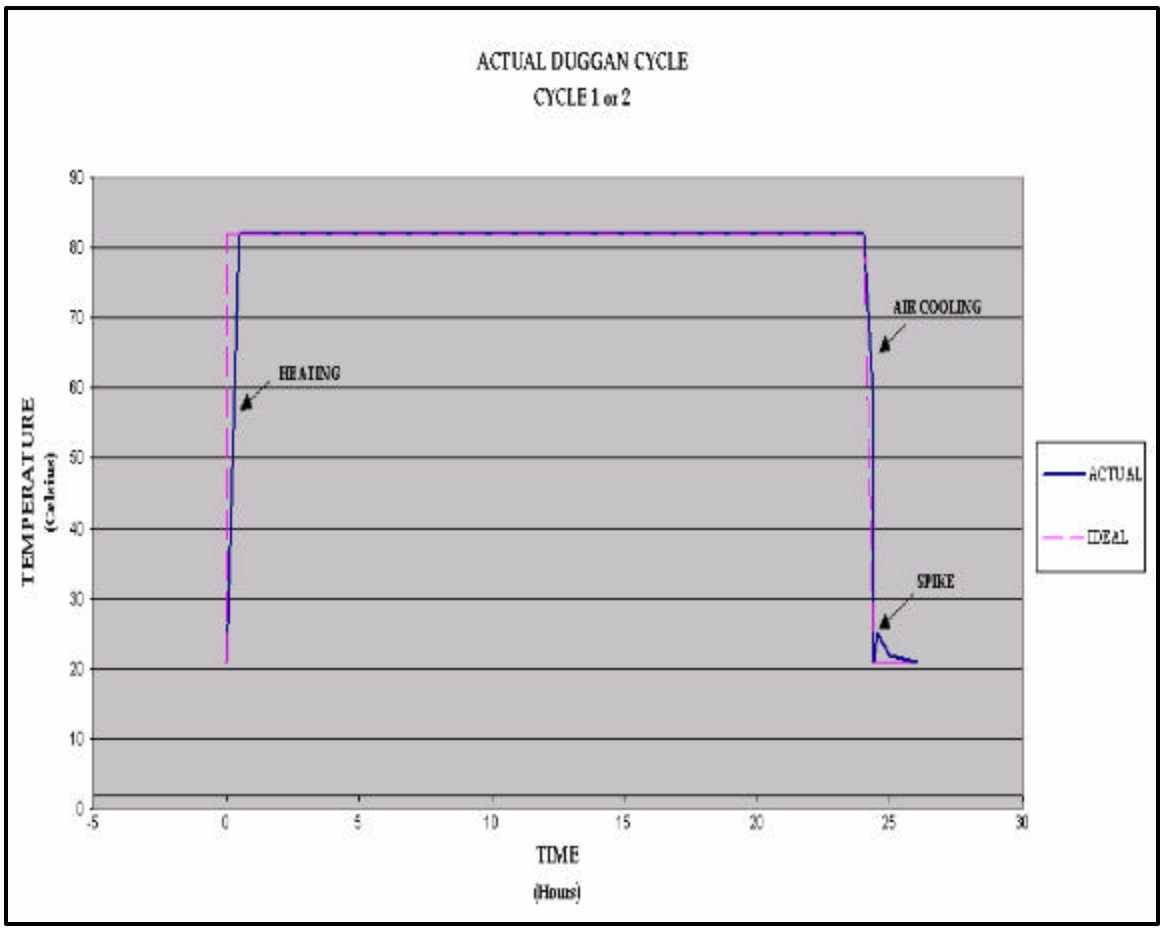

FIGURE 4.3 – Actual Duggan Heating Cycle

The temperature is tracked for one of the first two cycles of the Duggan heat regimen and graphed on top of the ideal curve above. The part of the graph labeled "Heating" refers to the ambient temperature inside the oven. During this experiment, it took no more than thirty (30) minutes to reach the maximum temperature. After air-cooling in the oven for approximately forty-five (45) minutes, the ambient temperature had dropped to 57° C. Air-cooling reduced the temperature gradient of the water-cooling and thus excessive cracking of the samples was avoided. The part of the graph labeled "spike" refers to the temperature of the water bath after placement of the hot samples. To reduce this effect, the volume of the water bath should be increased or the number of hot samples per bath should be limited.

FIGURE 4.4 – Sampling SEM Specimens

Fractured surfaces were used as SEM specimens. Two (2) specimens were collected from each sample set, "EXTERIOR" and "INTERIOR". This distinction was made for documentation purposes and not for a statistical analysis. SEM results were used qualitatively (Shown: Prism segments and regions of sampling inside a prism segments. All exterior specimens shared a side in common with the outside surfaces of the prism, therefore easily making them distinguishable from the interior samples taken from the middle of the prism.)

FIGURE 4.5 – Mounting of Fractured Surfaces

The fractured surfaces were mounted on half (1/2) inch diameter carbon discs using carbon paint and dried in a vacuum oven at 55° C. The discs were used to mount the surfaces in the SEM specimen chamber. Carbon is useful for this purpose since, as a conductive material, it minimizes charging effects. Static charges on the surface will appear as bright spots in the SEM image. The carbon works by conducting away the charges that would otherwise buildup on the surface. The carbon mounting and paint does not affect the results since the SEM is configured to ignore carbon in its elemental analysis or spectrum. (Shown: A fractured surface is mounted on a black carbon disc using the conductive carbon paint displayed in the background. Corks are used as a stand for the discs.)

FIGURE 4.6 – Carbon Coating of Fractured Surfaces

Fractured surfaces were coated with a film of carbon approximately 100 Angstroms thick to insure electrical conductivity and thus prevent charging effects in the microscope. (Shown: Fractured surfaces mounted inside a carbon-sputtering machine. The carbon film emits from a charged carbon electrode. The electrode glows white-hot as a 60 ampere current is past through it momentarily. Before the coating air inside the chamber is evacuated and replaced with argon gas. The ideal gas pressure inside the chamber is approximately 0.100 Torr).

CHAPTER 5 – Test Data Presentation

5.1 Compression Test Results Summary

None of the cylinders reached the design 28-day compressive strength of 5,000 psi. Thus water curing may have resulted in lower than expected strength. However, the dry Millville cylinders increased in strength with an average 270-day compressive strength in excess of 6,000 psi. The remaining cylinders lost as much as 85% of their original compressive strength. The compressive strength reported for each sample type is an average of three (3) compression tests (see Table 5.1). Compression results per sample type follow in sections 5.2.1 to 5.2.3. A cylinder's storage condition significantly affected the compressive strength. Despite sample type, all submerged cylinders experienced the largest reduction in strength between the 28-day and 270-day compression tests.

5.1.1 Compressive Strength of Silver Hill (Batch #1) Cylinders

Silver Hill cylinders experienced the second largest reduction in compressive strength between the 28-day and 270-day tests for both submerged and super saturated (fog) conditions with 82% and 71% reduction in strength respectively. Only Brandywine experienced a larger reduction. The submerged Silver Hill cylinders suffered the largest radial strain with an average diameter at the time of the 270-day compression test of 4.08 inches. It is here noted that submerged Silver Hill prisms suffered the largest linear strain.

5.1.2 Compressive Strength of Millville (Batch #2) Cylinders

The submerged exposure condition had a significant impact on the compressive strength of Millville cylinders. Between the 28-day and 270-day compressive strength tests, a 75% reduction in strength was recorded. Though the fog condition seemingly did not have a significant impact with only 6%

reduction in strength. The dry Millville cylinders experienced a gain in compressive strength of 28%.

5.1.3 Compressive Strength of Brandywine (Batch #3) Cylinders

Brandywine cylinders experienced the largest reduction in compressive strength between the 28-day and 270-day tests for both submerged and super saturated (fog) conditions with 85% and 86% reduction in strength respectively. The wetness of both exposure conditions seemed to affect the samples equally with nearly equal reduction in strength.

5.2 Linear Length Change Test Results Summary

Silver Hill prisms suffered the most linear expansion followed by Brandywine and Millville. The dry Millville prisms contracted.

The expansion results are presented per fine aggregate type in section 5.2.1 to 5.2.3. Plots of the all expansion data and expansion rate are presented in Figures 5.4 through 5.13. Ten (10) prisms were used to produce one (1) data point on the expansion curves. The variance of the first set of ten (10) measurements and the variance of the final set of ten (10) measurements was used to compute the average variance as plotted on the curves as error bars.

The expansion curves reflect weekly measurements taken between Sept. 20, 2002 to April 25, 2003. The period spanned a total of two hundred and ten (210) days.

The first derivative of each expansion curve was computed as an average rate between the weekly expansion measurements and plotted directly below the expansion graph for comparison purposes. The derivative plot shows the location of all inflection points on the expansion curve. The derivative plot also shows evidence supporting the theory that the expansion curves are approaching an asymptote and that expansion had all but stopped by the time of the last weekly expansion measurement on April 25, the only exception being the Silver

Hill samples. The expansion Silver Hill prisms seem to be continuing indefinitely.

5.2.1 Length Change of Silver Hill (Batch #1) Prisms

Submerged Silver Hill prisms suffered the most severe expansion of all samples with 0.63% total expansion. The maximum computed rate of expansion was 0.0092 in / day on day sixty-three (63). At the time weekly expansion measurements concluded, significant expansion was still being observed in the submerged samples. The last computed rate of expansion on day two hundred and ten (210) was 0.0002 in / day. The expansion of these samples seemed to continue indefinitely. No asymptotic behavior was found. The variance of the first set of ten (10) expansion measurements was 0.0018 and the variance of the final set was 0.0030 for an average variance of 0.0024.

Silver Hill prisms stored in fog suffered the most expansion among samples stored under supersaturated conditions with 0.47% total expansion. The maximum computed rate of expansion was 0.022 in / day on day ninety-one (91). At the time weekly expansion measurements concluded, significant expansion was still being observed in the supersaturated samples. The last computed rate of expansion on day two hundred and ten (210) was 0.00019 in / day. The expansion of these samples seemed to continue indefinitely. No asymptotic behavior was found. The variance of the first set of ten (10) expansion measurements was 0.00051 and the variance of the final set was 0.00119 for an average variance of 0.0009.

5.2.2 Length Change of Millville (Batch #2) Prisms

Submerged Millville prisms experienced the least expansion of all submerged samples with 0.12% total expansion. The maximum computed rate of expansion was 0.0035 in / day on day one hundred and five (105). At the time weekly expansion measurements concluded, no significant expansion was being

observed in the submerged samples. The last computed rate of expansion on day two hundred and ten (210) was $9.4x10^{-6}$ in / day. The expansion of these samples seemed to approach an asymptote near 0.12%. The variance of the first set of ten (10) expansion measurements was 0.0017 and the variance of the final set was 0.0015 for an average variance of 0.0016.

Millville prisms stored in fog experienced the least amount of total expansion among all samples with 0.05%. The maximum computed rate of expansion was 0.00089 in / day on day one hundred and five (105). At the time weekly expansion measurements concluded, no significant expansion was being observed in the supersaturated samples. The last computed rate of expansion on day two hundred and ten (210) was $1.0x10^{-6}$ in / day. The expansion of these samples seemed to approach an asymptote near 0.05%. The variance of the first set of ten (10) expansion measurements was 0.0015 and the variance of the final set was also 0.0015.

Dry Millville prisms contracted -0.038% during the period of weekly length change measurements. The contraction behavior was markedly different from that of expansion. The maximum dry contraction rate occurred much earlier than the maximum rates of expansion. On day twenty-eight (28) a maximum contraction rate of - 0.0014 in / day was computed. After the maximum was reached, the contraction rate rapidly decayed. Resulting in asymptotic behavior that approached a terminal value near 0.038% contraction. The last computed rate of contraction on day two hundred and ten (210) was $-1.5 x10^{-6}$ in / day. The expansion of these samples seemed to approach an asymptote near 0.05%. The variance of the first set of ten (10) expansion measurements was 0.0019 and the variance of the final set was also 0.0019.

5.2.3 Length Change of Brandywine (Batch #3) Prisms

Submerged Brandywine prisms suffered moderate expansion relative to the other submerged samples with 0.49% total expansion. The maximum

computed rate of expansion was 0.0097 in / day on day eighty-four (84). At the time weekly expansion measurements concluded, no significant expansion was being observed in the submerged samples. The last computed rate of expansion on day two hundred and ten (210) was $7.4x10^{-6}$ in / day. Thus supporting a strong tendency toward asymptotic behavior. The limiting value was near 0.49%. The variance of the first set of ten (10) expansion measurements was 0.00021 and the variance of the final set was 0.00026 for an average variance of 0.0023.

The Brandywine prisms stored in fog suffered moderate expansion relative to other samples with 0.26% total expansion. The maximum computed rate of expansion was 0.0046 in / day on day eighty-four (84). At the time weekly expansion measurements concluded, significant expansion was not being observed in the supersaturated samples. The last computed rate of expansion on day two hundred and ten (210) was $8.5x10^{-6}$ in / day. Thus supporting theory expansion of the samples was approaching a limiting value near 0.26%. The variance of the first set of ten (10) expansion measurements was 0.00067 and the variance of the final set was 0.00089 for an average variance of 0.00075.

5.3 SEM and EDAX Analysis Results

Table 5.2 summarizes the results of the SEM analysis of all thirty (30) fractured surfaces. The table contains information on were the sample came from and whether ettringite, ASR, or calcium hydroxide was found.

Generally, the results at least hinted at a direct correlation between water exposure and DEF or ettringite development in general. For example, dry Millville samples, the only sample set with the dry exposure condition, were not found with ettringite. While wet Millville samples, both submerged and supersaturated, were found with ettringite.

The occurrence of ASR gel was rare compared to that of ettringite or calcium hydroxide. Only one instance of ASR gel was confirmed by both a photograph and an EDAX spectrum.

5.4 Discussion of The Kinetics of Expansion and The Damage Process

The influence of ASR rating on expansion and damage is summarized in Table 5.3. The expansions at 200 days qualitatively agreed with the ratings from the MDSHA ASR test. Silver Hill with highest ASR test rating had the greatest expansion while Millville with the lowest ASR test rating had the lowest expansion, had the smallest expansion, and Brandywine fell in between. This ranking was the same for both submerged and fog moisture conditions. Conversely, Millville had the highest compressive strength for both cases. However, Brandywine, instead of Silver Hill, had the lowest compressive strengths. It should be noted that in the submerged case, the difference between the two might not be statistically significant. These results indicate that expansion tests alone are not an infallible predictor of actual concrete durability as measured by long term compressive strength

Considering the kinetics of expansion, there was a clearly identifiable main peak in each case, except for Brandywine stored in fog. This peak occurred significantly earlier in Silver Hill than the others for both moisture conditions. Since the timing of the peak depends mainly on the kinetic rate constant (Livingston, 1998), this implies that the Silver Hill aggregate is more reactive. The peak in Silver Hill occurs at 60 days. This also suggests an alternative method of defining the expansiveness ratings of aggregates. Instead of using the amount of expansion at an arbitrary fixed time, for example 16 days in ASTM C1260, one could use the time of the peak, which is physically more meaningful.

The shape of the expansion curves usually exhibits a very slow expansion initially. The curve for the Millville prisms stored in dry air shows significant

shrinkage during this early period. There are at least three components to shrinkage: drying, thermal and autogenous or chemical. Given the time delay between casting and the start of initial measurement, thermal shrinkage would be negligible in these data. Thus the observed shrinkage is a combination of drying and chemical shrinkage. Both of these concern the demand for water in the curing concrete. Since the shrinkage curve levels out just when the moist storage curves take off, this suggests that in the latter the chemical shrinkage dominates over the expansive processes in the consumption of water from external sources. It is only when the chemical shrinkage is largely completed, that the expansive processes take over. Only chemical shrinkage is important here, since drying shrinkage by definition could not happen in submerged or 100% RH conditions.

Contrasting the submerged and the fog-stored cases reveals some interesting differences. Both Millville and Silver Hill showed much reduced compressive strengths for the submerged cases compared to the fog case. However, Brandywine, which had the lowest compressive strengths, showed no statistically significant difference. To understand this, it is necessary to consider the processes that control the rate of reaction of the water. First, it must physically pass from the outside into the concrete, which is a physical mass transfer, or diffusion-limited, process. Then it must chemically react to generate expansive products. The diffusion rate into the concrete should be much lower for the fog case since the surface concentration of water molecules is orders of magnitude lower. The fact that Brandywine compressive strength is insensitive to this difference indicates that in it the processes are controlled by chemical reactions, or in essence the rate of reaction is slower than the rate of delivery of water. Conversely, the compressive strengths of the other two mixes show considerable sensitivity to mass transfer conditions; hence the chemical reactions must be faster than the diffusion processes.

This is also borne out in the expansion rate data. The time of the peak shifts significantly for the Silver Hill and Millville mixes, but not for the Brandywine.

Note that these differences among the aggregate types involve both physical and chemical aspects. As shown in the schematic diagram below, the overall damage process involves several steps. The water has to physically transfer into the concrete, a diffusion-controlled process. Then it has to chemically react with the aggregate, creating expansive stresses, and finally the stresses produce an expansive strain of the material depending on its constitutive

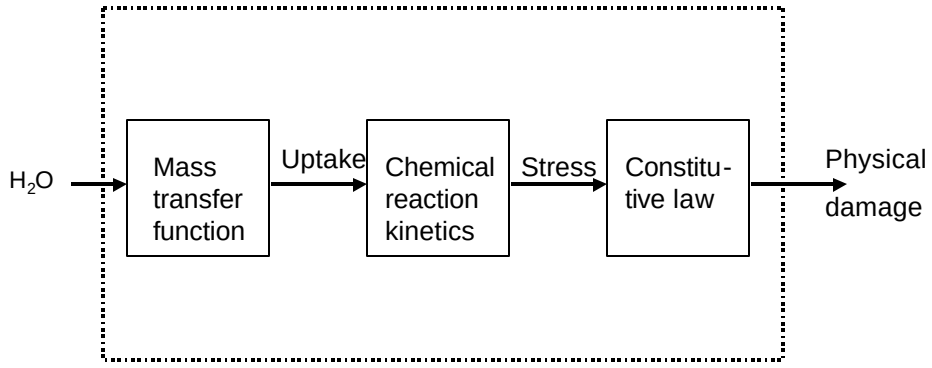

Schematic diagram of damage process

law (Livingston, 2004). The diffusion rate is mainly determined by the microstructure of the cement paste in terms of pore size distribution and connectivity. These in turn depend upon the grain-size distribution of the fine aggregate and its reactivity with the Portland cement. The chemical reaction rate depends upon the specific surface of the fine aggregate and its reaction rate with water molecules.

The shapes of the expansion curves also show differences between the two storage conditions. For Silver Hill, the two curves have effectively the same

shape up to 100 days, but the fog curve appears to be lagging in time, which would be a reflection of the slower water transport. The Millville mix also seems to show a small time lag for the fog case, but the slopes of the two curves differ. However, the Brandywine curves show no time lag. The two curves coincide up to 75 days.

A major and unavoidable problem in DEF research is the lack of a reliable analytical method for quantifying the amount of ettringite present. This arises because the mineral form of ettringite, as distinct from monosulfate or gypsum, must be explicitly identified in the cement paste regions that are randomly distributed around fine and coarse aggregate particles. The available methods are powder X-ray diffraction, thermogravimetric analysis (TGA) and scanning electron microscopy (SEM) with energy dispersive X-ray diffraction (EDXRD). These all are limited to very small volume of sample, on the order of 10 mm^3, that may not be representative of the overall volume of the prism. Moreover, quantitative X-ray diffraction requires extensive and painstaking sample presentation, but even then may not be sensitive to minerals that are present in amounts of less than 1% (Stutzman, 1996). TGA is a more robust method, but the ettringite may be interfered by the presence of other phases. The SEM method relies upon visual identification of the characteristic ettringite crystal shape in the image. However, the image area is only on the order of 100 by 100 μm, which makes it essentially impossible to carry out an exhaustive examination of the sample. Consequently, in the following discussion it should be understood that the results are qualitative.

Ettringite was found by SEM fracture surface analysis in all three batches that were stored in water at 9 months. (Table 5.2). For the submerged cases, there appears to be a trend toward more expansion as the frequency of ettringite observations increases. Several morphologies of ettringite were observed, with lamellar structures developing at later times. This is consistent with observations

from the cores taken from Maryland bridges in which the lamellar structure developed with more advanced damage.

Finally, although ettringite was frequently observed, there was only one SEM sample that contained ASR gel. The implication is that expansion tests do not measure ASR effects only, but rather the combined effects of ASR, DEF and moisture absorption.

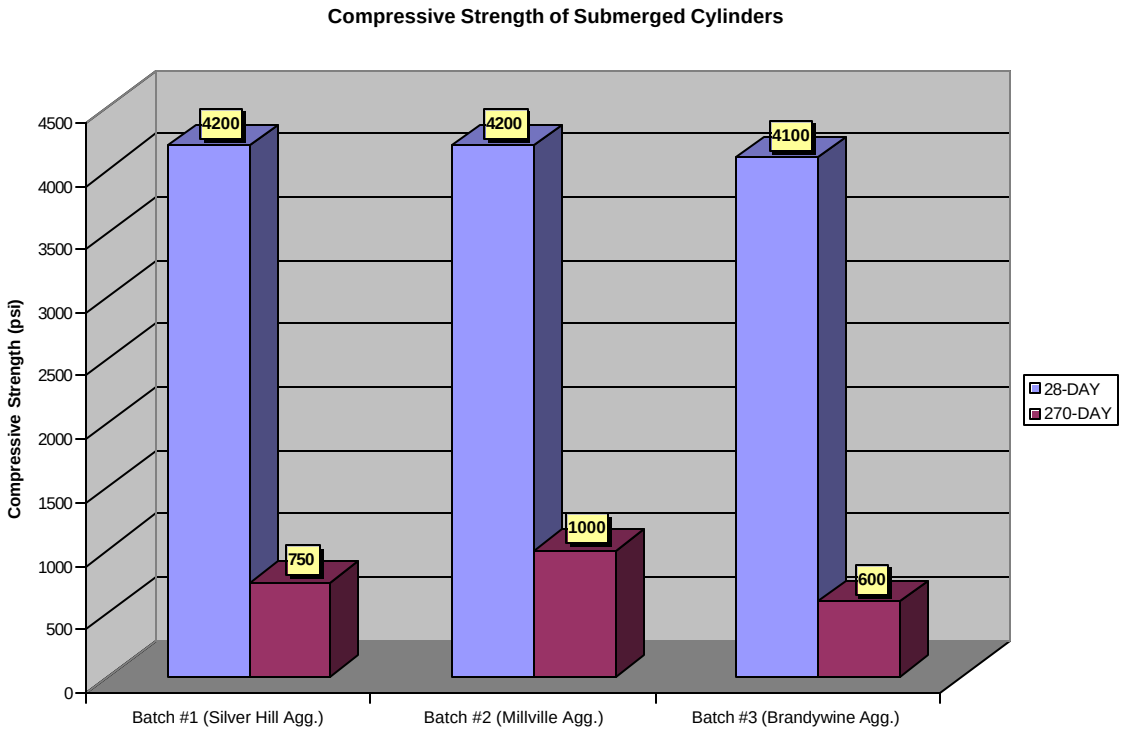

FIGURE 5.1 – Compressive Strength of Submerged Cylinders

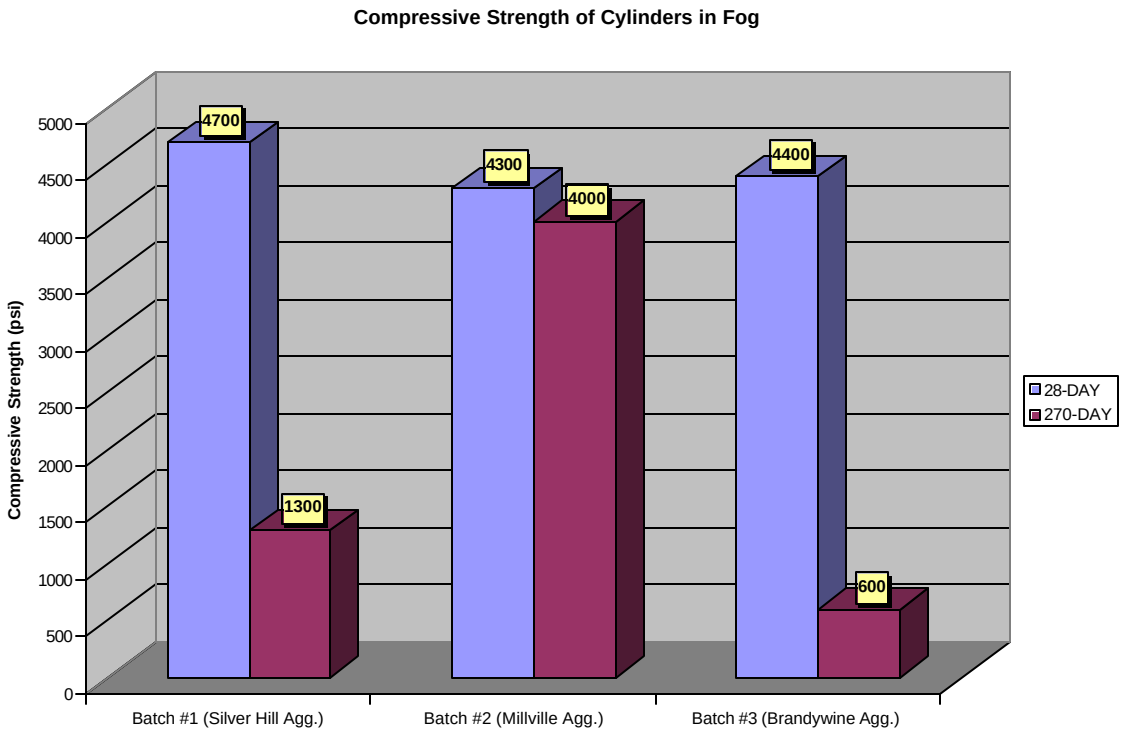

FIGURE 5.2 – Compressive Strength of Cylinders in Fog

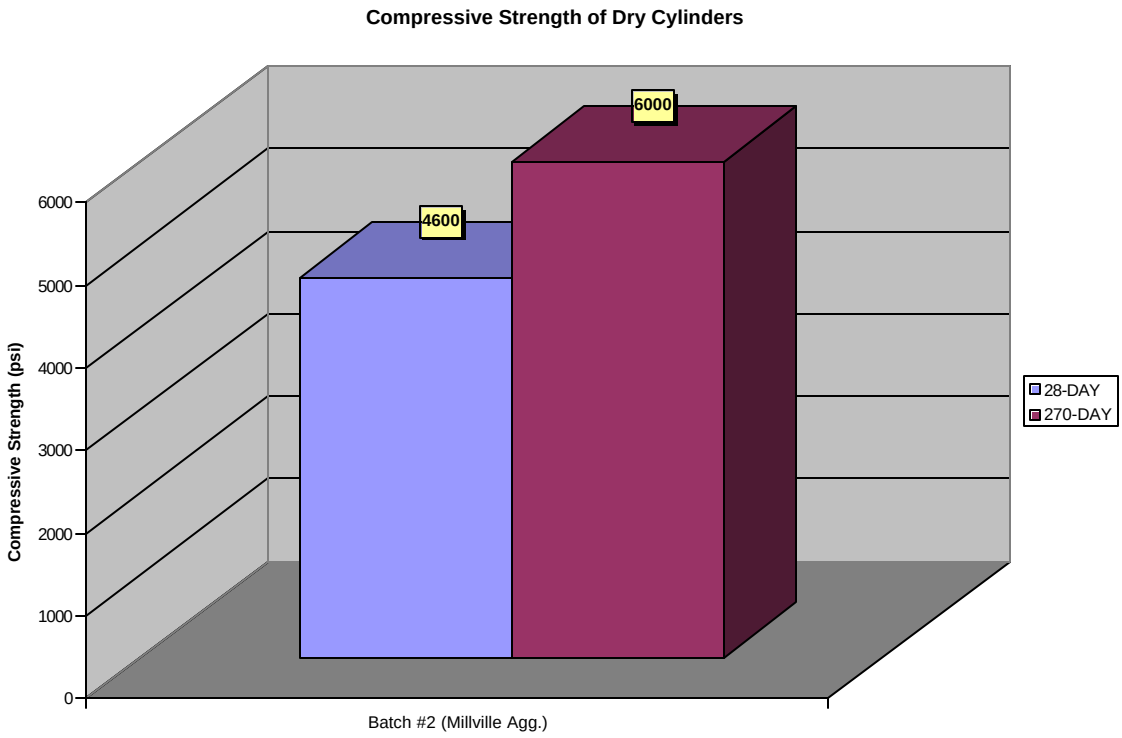

FIGURE 5.3 – Compressive Strength of Dry Cylinders

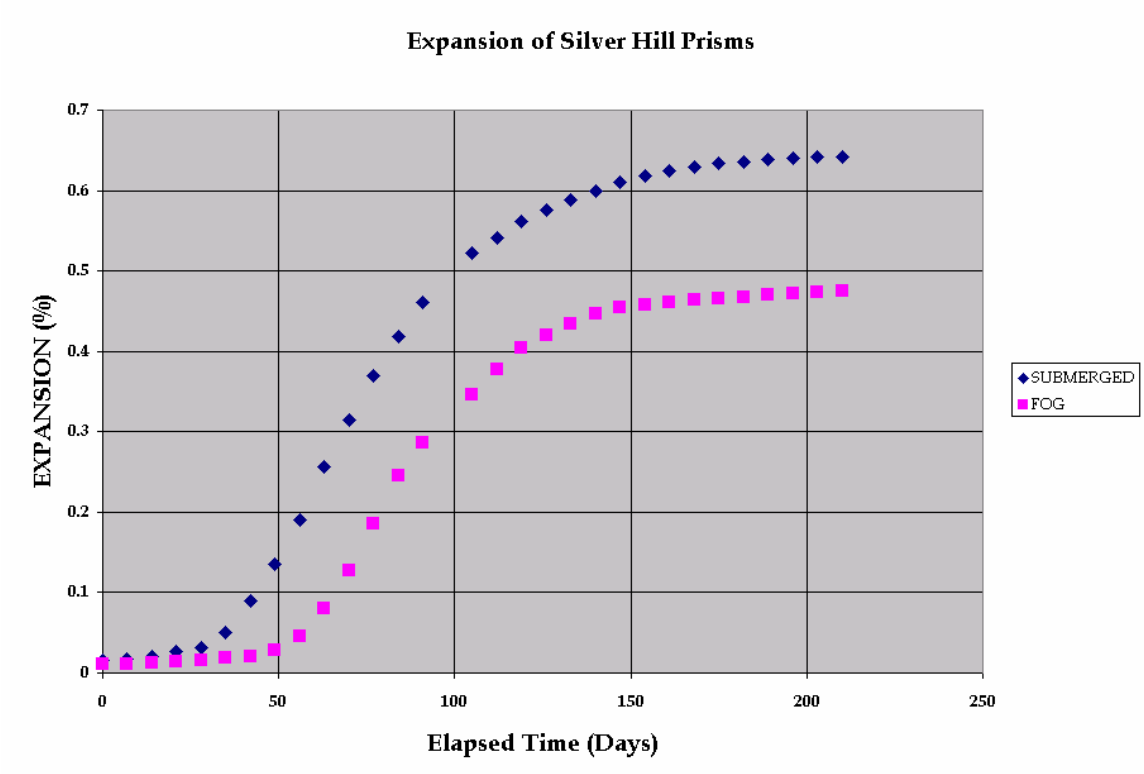

FIGURE 5.4 – Summary of Expansion of Silver Hill Prisms

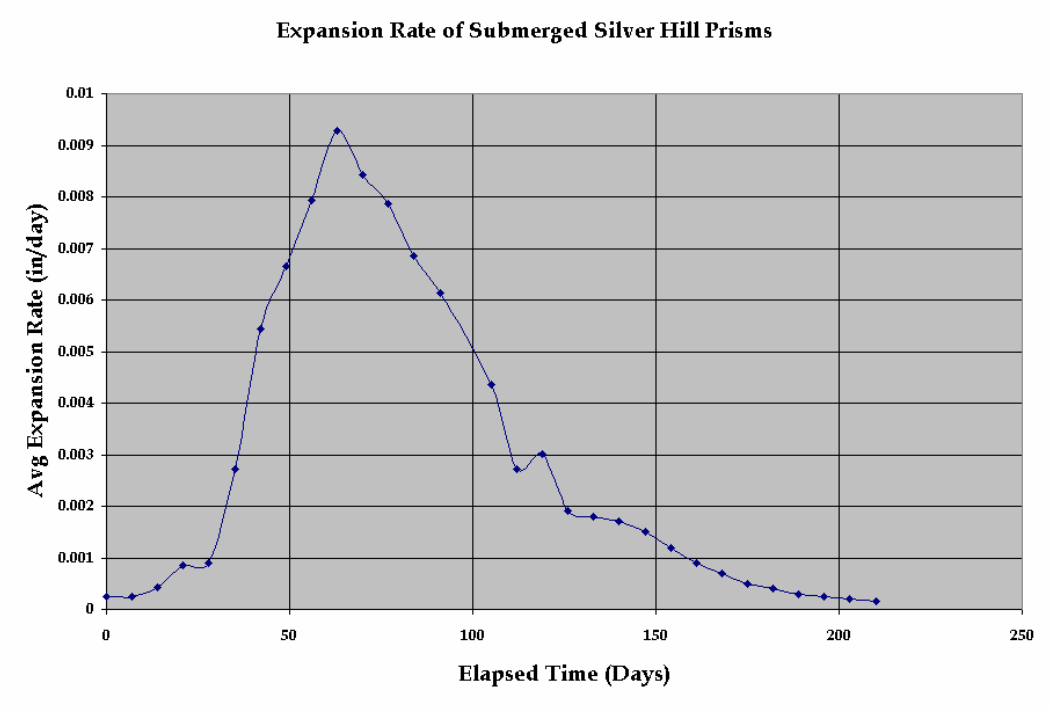

FIGURE 5.5 – Expansion Rate of Submerged Silver Hill Prisms

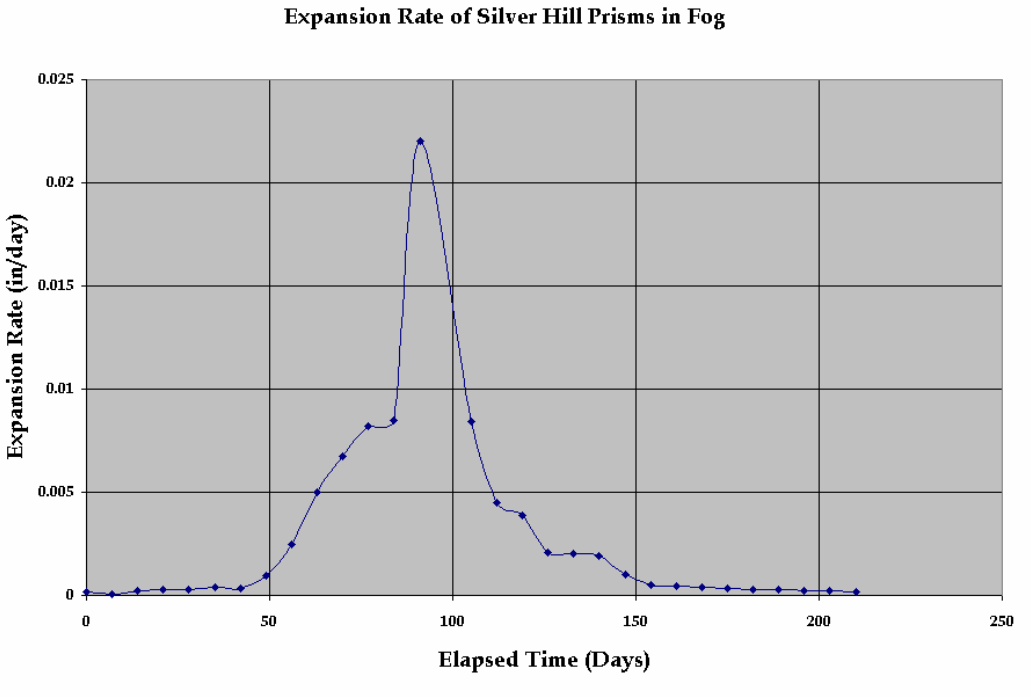

FIGURE 5.6 – Expansion Rate of Silver Hill Prisms in Fog

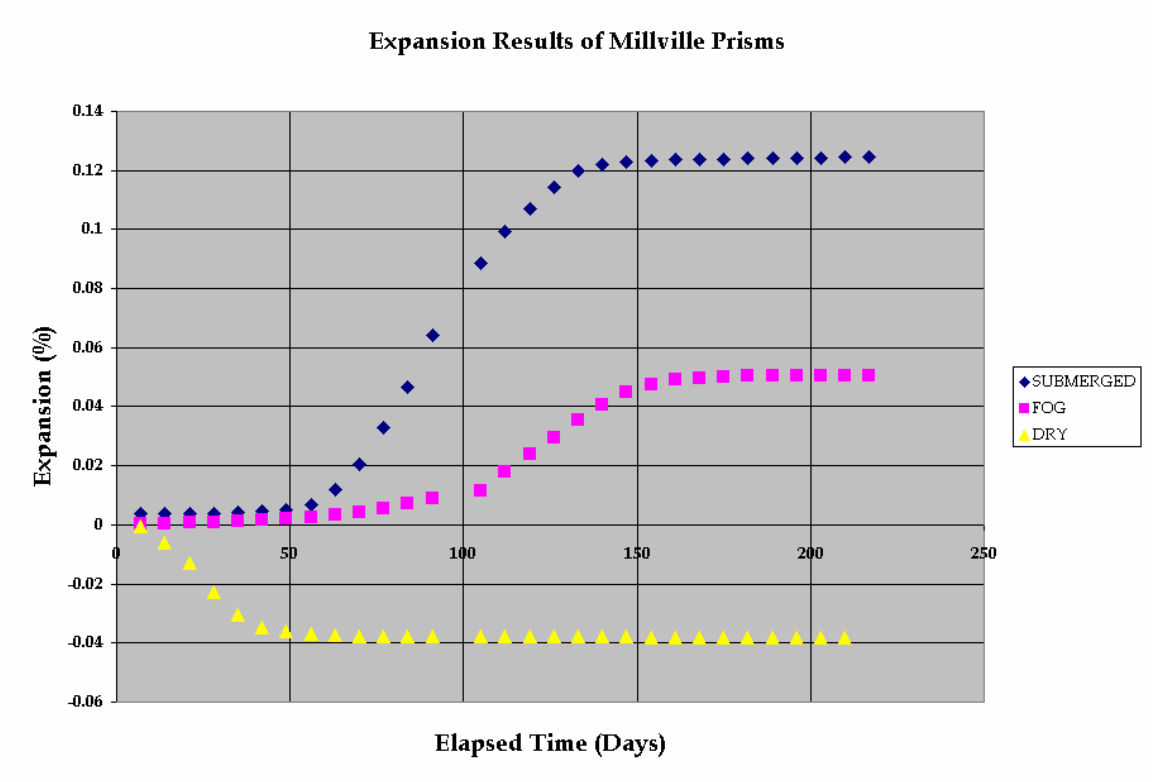

FIGURE 5.7 – Summary of Expansion of Millville Prisms

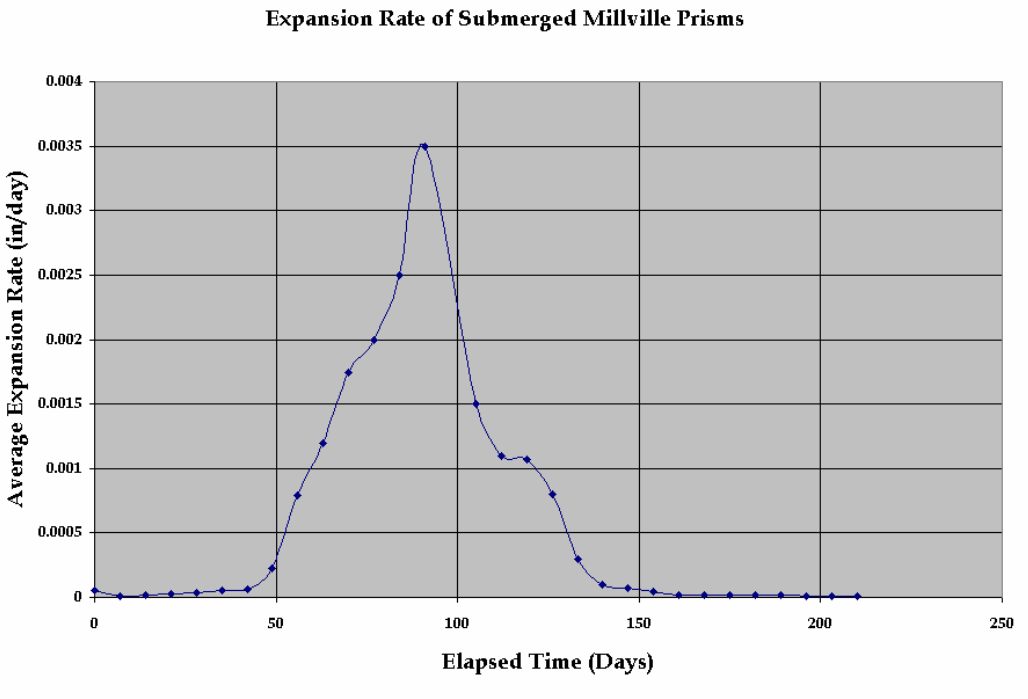

FIGURE 5.8 – Expansion Rate of Submerged Millville Prisms

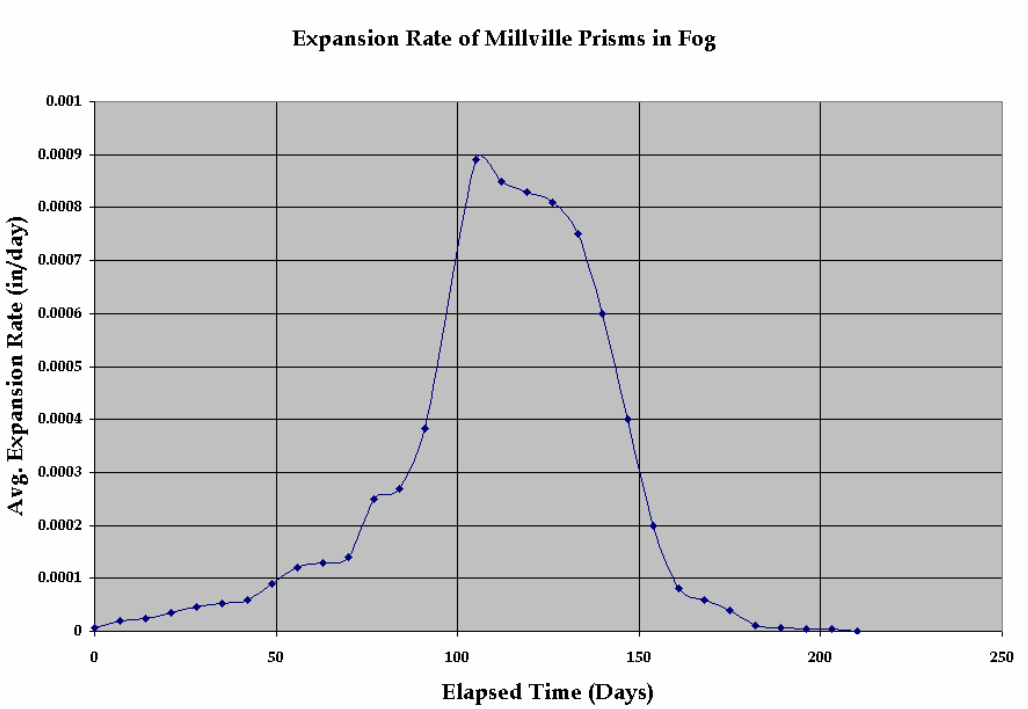

FIGURE 5.9 – Expansion Rate of Millville Prisms in Fog

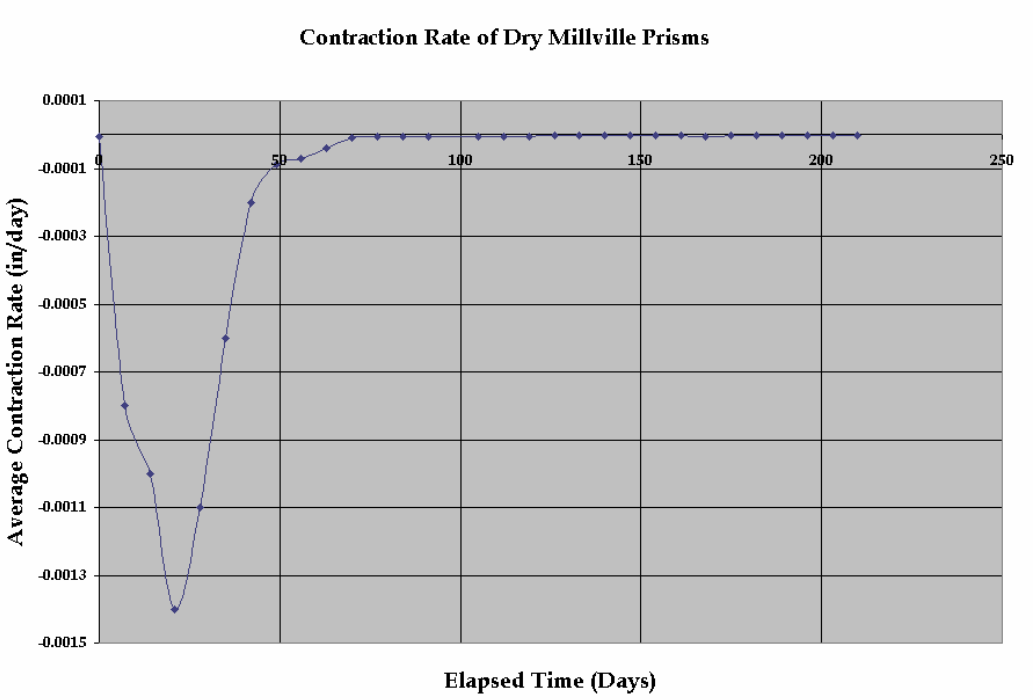

FIGURE 5.10 – Expansion Rate of Dry Millville Prisms

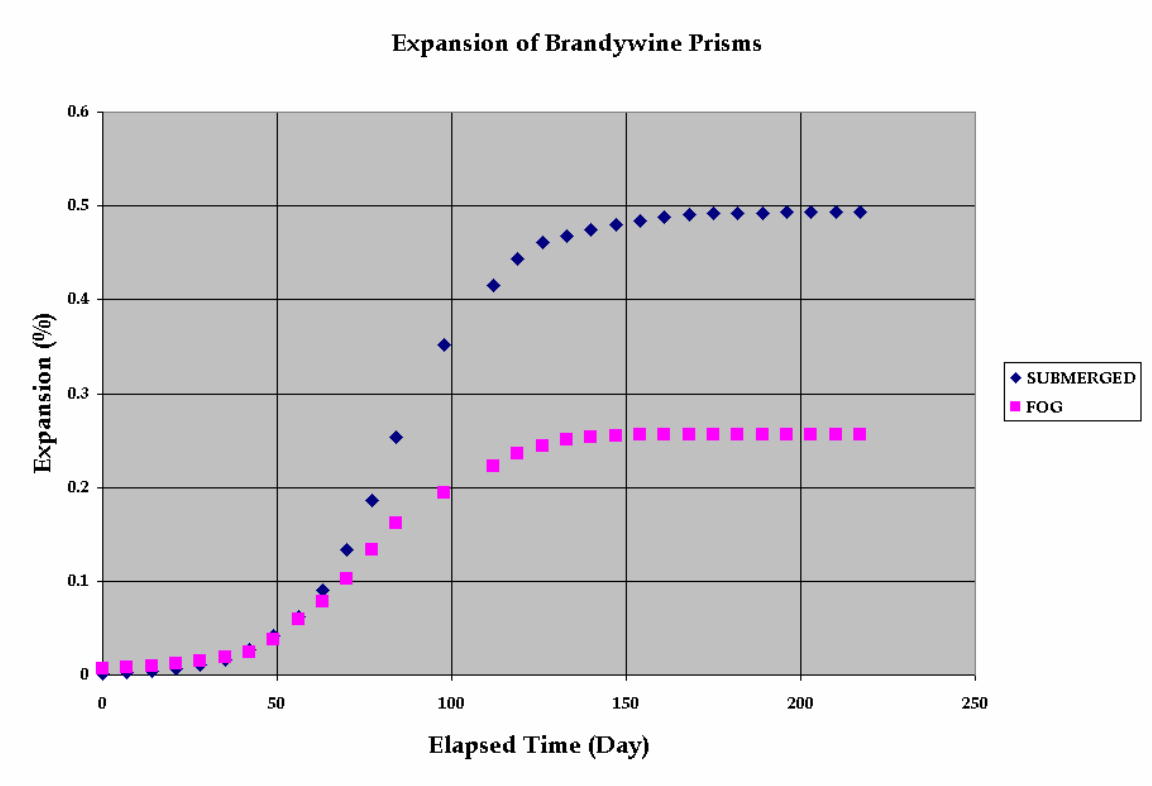

FIGURE 5.11 – Summary of Expansion of Brandywine Prisms

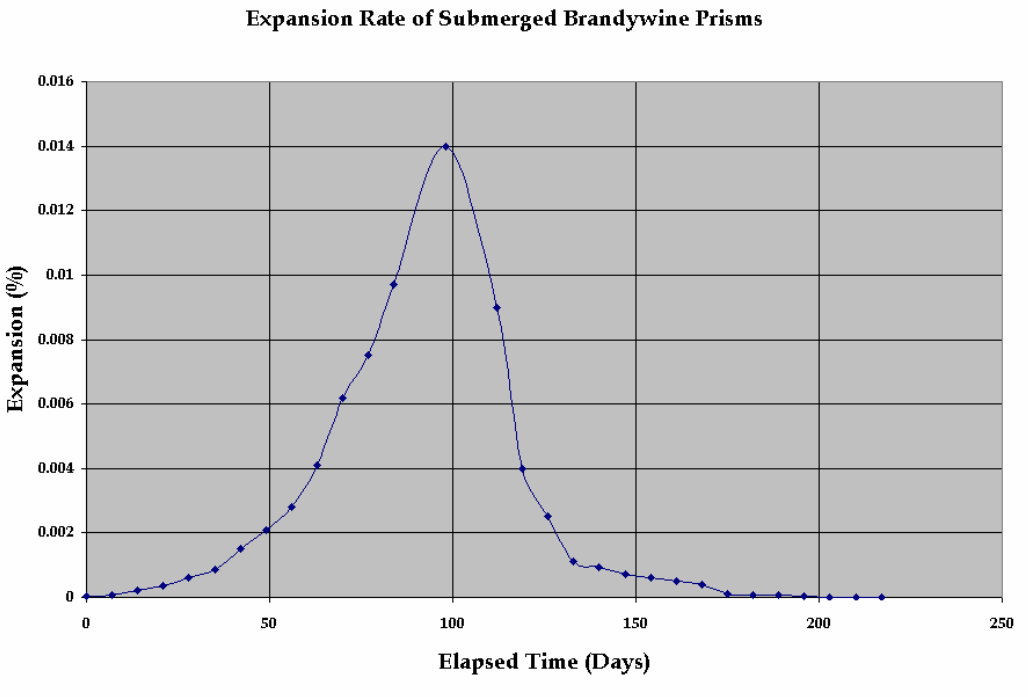

FIGURE 5.12 – Expansion Rate of Submerged Brandywine

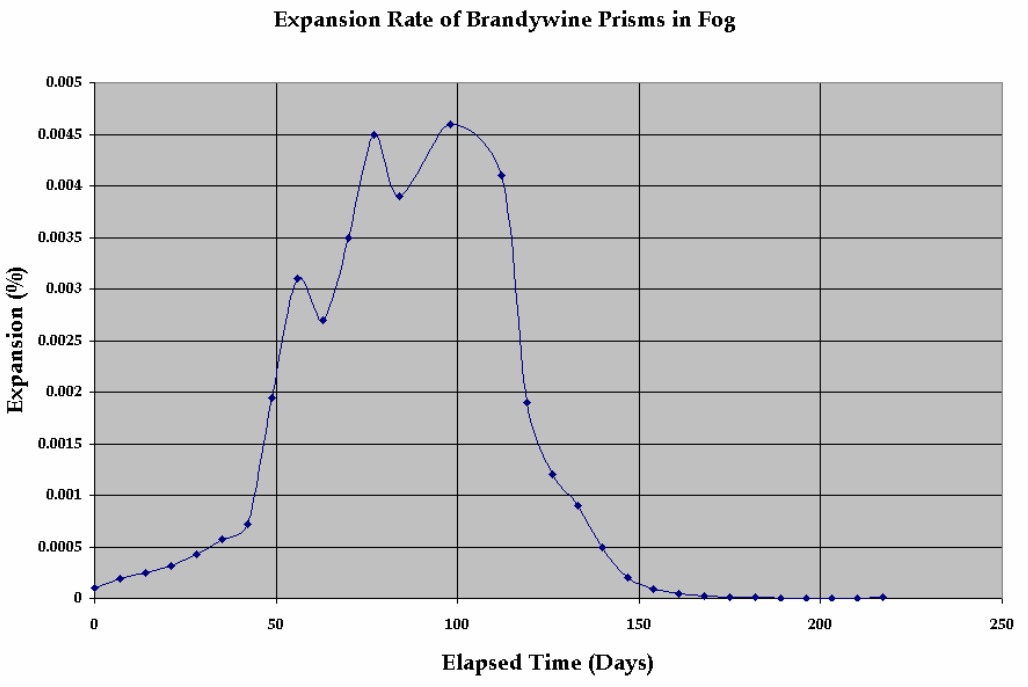

FIGURE 5.13 – Expansion Rate of Brandywine Prisms in Fog

TABLE 5.1 – **COMPRESSIVE STRENGTH**

	Batch # 1 Silver Hill Agg.		**Batch # 2 Millville Agg.**		**Batch # 3 Brandywine Agg.**	
Exposure Condition	28 Day Strength (psi)	270 Day Strength (psi)	28 Day Strength (psi)	270 Day Strength (psi)	28 Day Strength (psi)	270 Day Strength (psi)
Submerged	4,200 ± 140	750 ± 80	4,200 ± 54	1,000 + 100	4,100 ± 240	600 ± 130
Fog	4,700 ± 160	1,300 ± 500	4,300 ± 78	4,000 ± 82	4,400 ± 250	600 ± 130
Dry	-----	-----	4,600 ± 63	6,000 ± 300	-----	-----

TABLE 5.2 – SEM and EDAX Analysis Results Summary

SAMPLE ID#	AGG.	EXPOSURE	LOCATION	TEST DATE	AGE*	ETTRINGITE	ASR	CALCIUM HYDROXIDE	OTHER
1146	MILLVILLE	SUB.	INTERIOR	2/11/2003	6 MO.	PROB.		PROB.	
1147	MILLVILLE		EXTERIOR						
1148	BRANDYWINE		INTERIOR						
1149	BRANDYWINE		EXTERIOR	2/20/2003		PROB.			
1150	SILVER HILL		INTERIOR						
1151	SILVER HILL		EXTERIOR			POS.		PROB	
1152	SILVER HILL	SUB.	INTERIOR	5/13/2003	9 MO.				
1153	SILVER HILL		EXTERIOR			PROB.			CAL. CARB.
1154	SILVER HILL	FOG	INTERIOR	5/15/2003			POS.		
1160	SILVER HILL		EXTERIOR						
1161	BRANDYWINE	SUB.	INTERIOR			PROB.	PROB.		CAL. CARB.
1162	BRANDYWINE		EXTERIOR	5/20/2003					
1163	BRANDYWINE	FOG	INTERIOR	6/5/2003			PROB.		
1164	BRANDYWINE		EXTERIOR						
1165	MILLVILLE	SUB.	INTERIOR	6/18/2003		PROB.			
1166	MILLVILLE		EXTERIOR	6/10/2003		PROB.			
1167	MILLVILLE	FOG	INTERIOR						
1168	MILLVILLE		EXTERIOR						
1169	MILLVILLE	DRY	INTERIOR	6/25/2003					
1171	MILLVILLE		EXTERIOR						
1172	SILVER HILL	SUB.	INTERIOR	7/2/2003	4 WKS				
1173	SILVER HILL		EXTERIOR	7/13/2003		POS.			
1174	MILLVILLE		INTERIOR			PROB.		POS.	
1175	MILLVILLE		EXTERIOR	7/12/2003				POS.	
1176	BRANDYWINE		INTERIOR	7/19/2003		PROB.			
1177	BRANDYWINE		EXTERIOR						
1178	MILLVILLE	DRY	INTERIOR	7/27/2003					
1179	MILLVILLE		EXTERIOR						
	SILVER HILL	N/A	INTERIOR	8/2/2003	1 DAY				
	SILVER HILL		EXTERIOR			PROB.			

The figure above tracks the occurrence of ettringite, ASR gel, calcium hydroxide, and calcium carbonate (CAL. CARB.) on the fracture surfaces. If just a photograph was available for the site, the occurrence was listed as probable (PROB.). If both a photograph and an EDAX spectrum were available for the site, the identification was considered positive (POS.).

*Age of the sample when it was first removed from its intended exposure condition.

Table 5.3 - Influence of ASR Rating on Expansion and Damage

	Batch #1 Silver Hill Agg.		**Batch #2 Millville Agg.**		**Batch #3 Brandywine Agg.**	
ASR Rating	0.28		0.028		0.14	
Exposure Condition	Sub-merged	Fog	Sub-merged	Fog	Sub-merged	Fog
Expansion @ 200 days	0.64	0.48	0.125	0.05	0.49	0.26
Compressive Strength @ 270 days (psi)	750 ± 80	1,3000 ± 500	1,000 ± 100	4,000 ± 82	600 ± 130	600 ± 130
Peak Expansion Rate	0.0093	0.23	0.0035	0.0009	0.014	0.0046
Time for Peak Expansion Rate (Days)	60	90	90	110	98	100

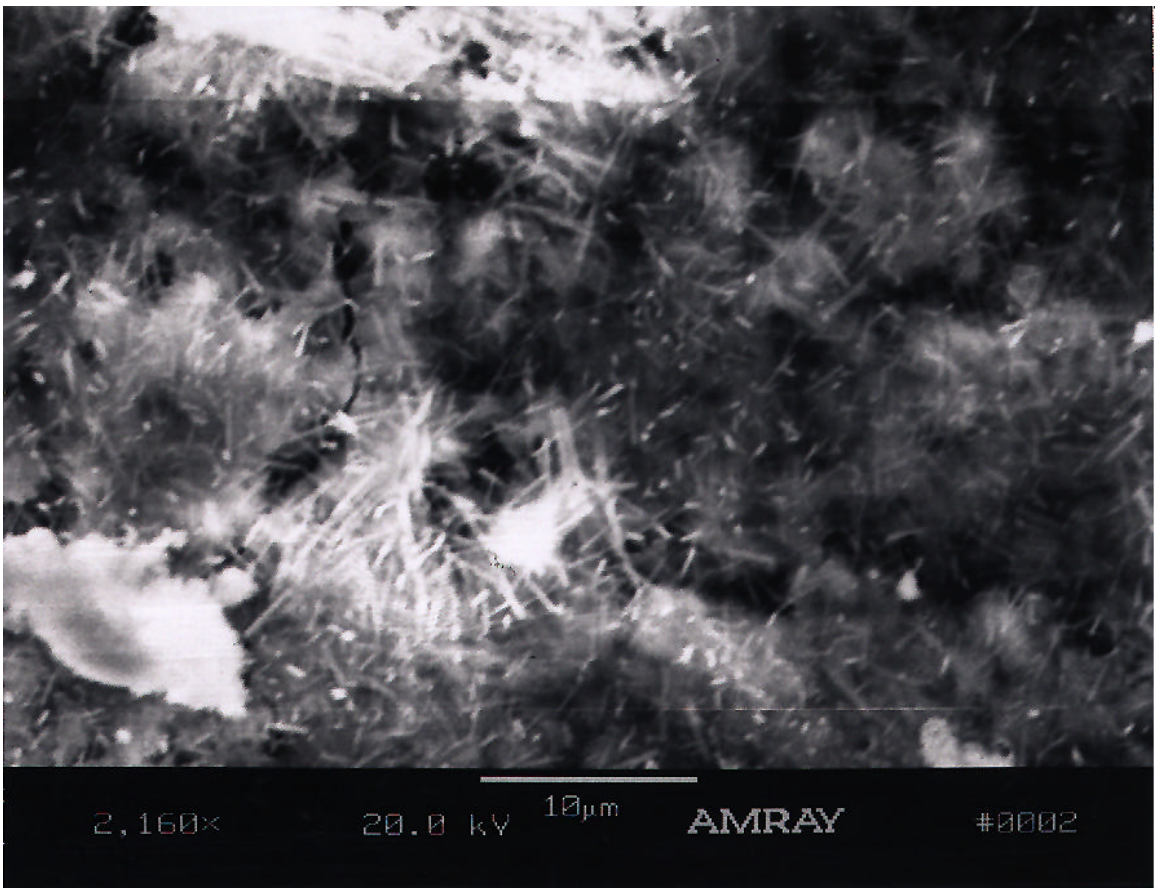

FIGURE 5.14 – Ettringite as a Product of Hydration

An SEM examination of fresh mortar samples reveals ettringite as it forms during hydration. The fine needle shaped crystals of ettringite shown above was found on an exterior piece from a mortar cube made with Silver Hill sand one (1) day after casting. The size of ettringite that forms as a product of hydration may depend on cement chemistry [Stark, J. and Bollmann, K., 1997]. The fine ettringite needles above contrast with the larger coarse crystals, which may also form during cement hydration.

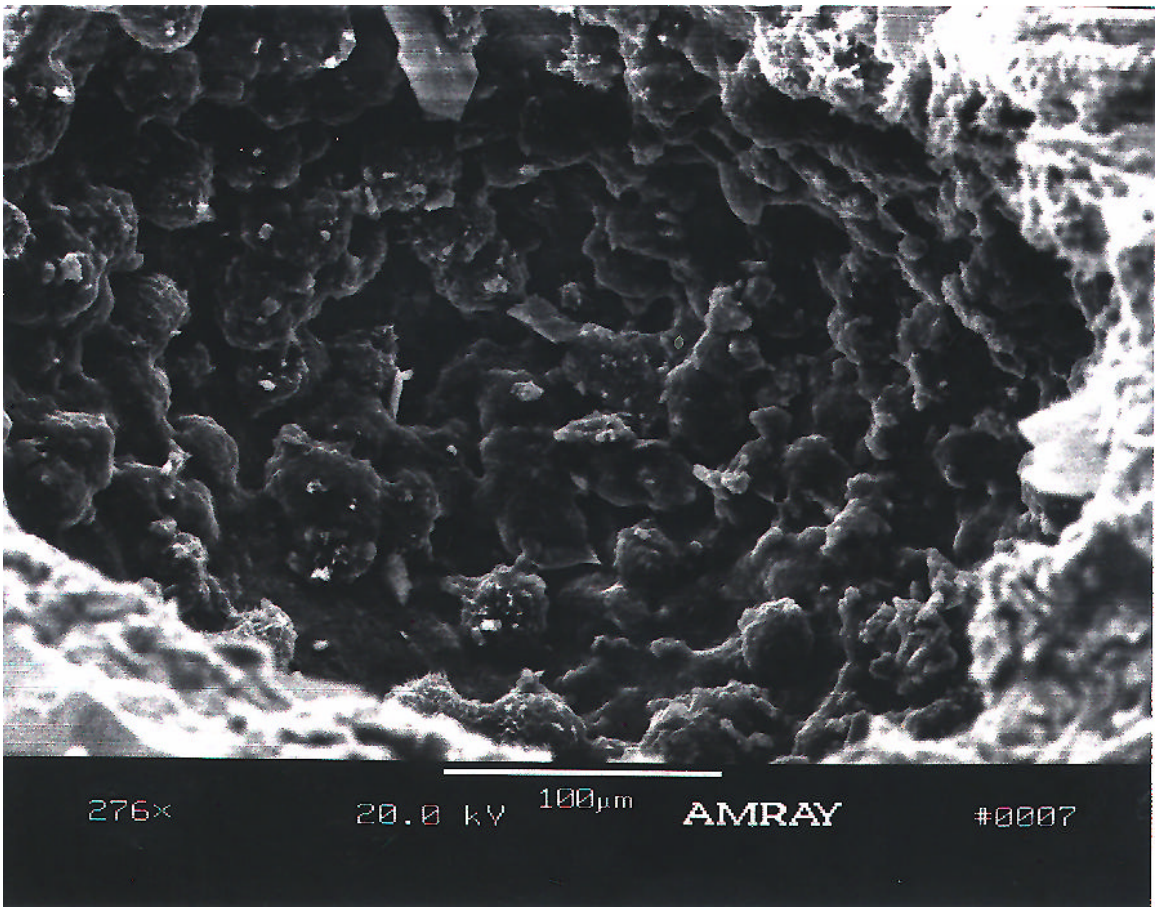

FIGURE 5.15 – Amorphous Calcium Aluminum Sulfate in Concrete

The amorphous formation shown above is suspected of being calcium aluminum sulfate (the term ettringite applies primarily to the crystalline form). The photograph is of an interior fragment taken from a Silver Hill prism four (4) weeks after casting. The site is located at a 'pullout' or place were the coarse aggregate interfaced with the cement paste. No EDAX spectrum is available for the site. The identification is based on geometry and past experience examining concrete with the SEM.

FIGURE 5.16 – Lamellar Ettringite with Complex Structure

The lamellar or blade-like ettringite shown above was found on an exterior fragment of a one (1) year old Silver Hill prism. The site is a 'pullout'. No EDAX analysis is available for the site. Probable identification is based on the geometry of the suspected ettringite and past experience examining concrete using the SEM. Lamellar ettringite was found in only samples aged for at least one (1) year.

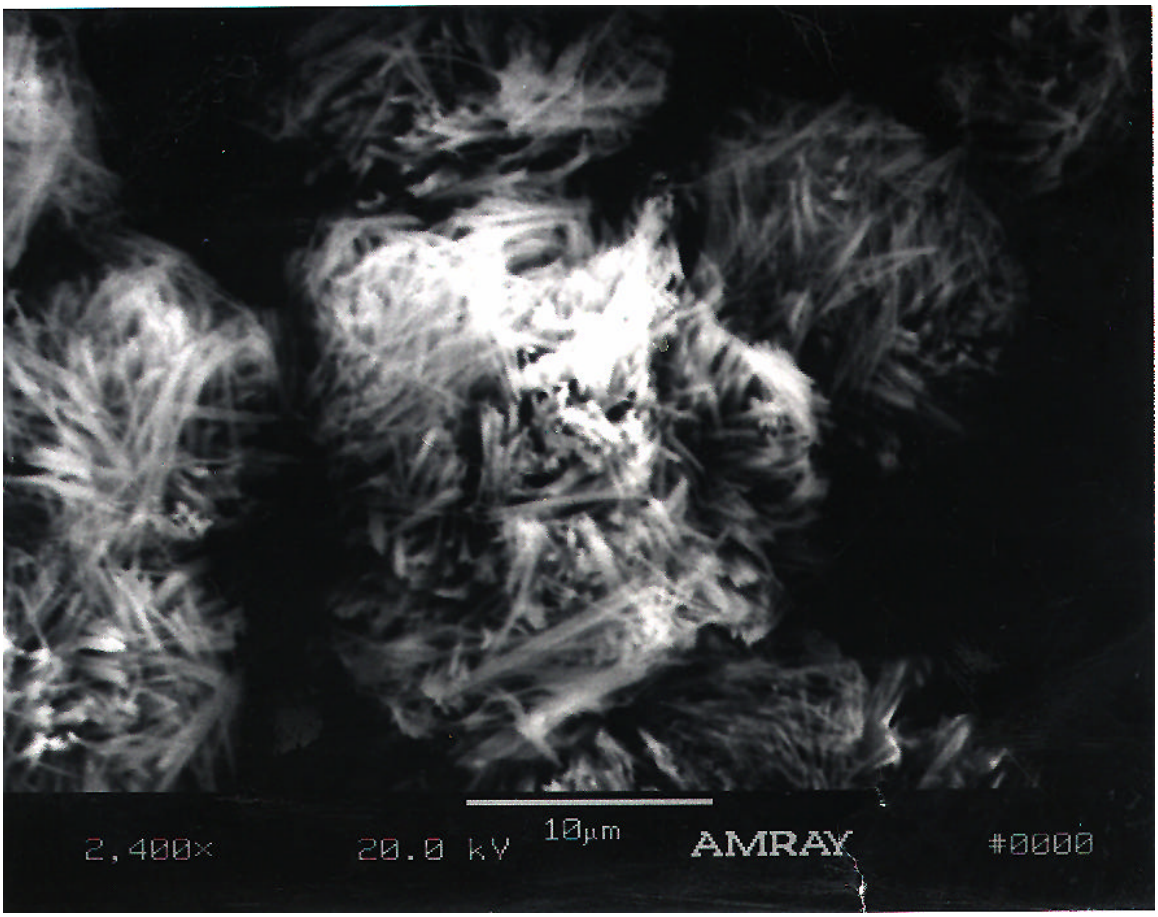

FIGURE 5.17 – Ettringite Bundles in Heat Treated Concrete

Bundles of ettringite were commonly found in heat-treated concrete samples. The photograph above is of an interior fragment taken from a Brandywine prism four (4) weeks after casting. The prism was stored in fog. Most likely the site is an air void. No EDAX analysis of the site is available. The probable identification is based on the geometry of the suspected ettringite and past experience examining concrete with the SEM.

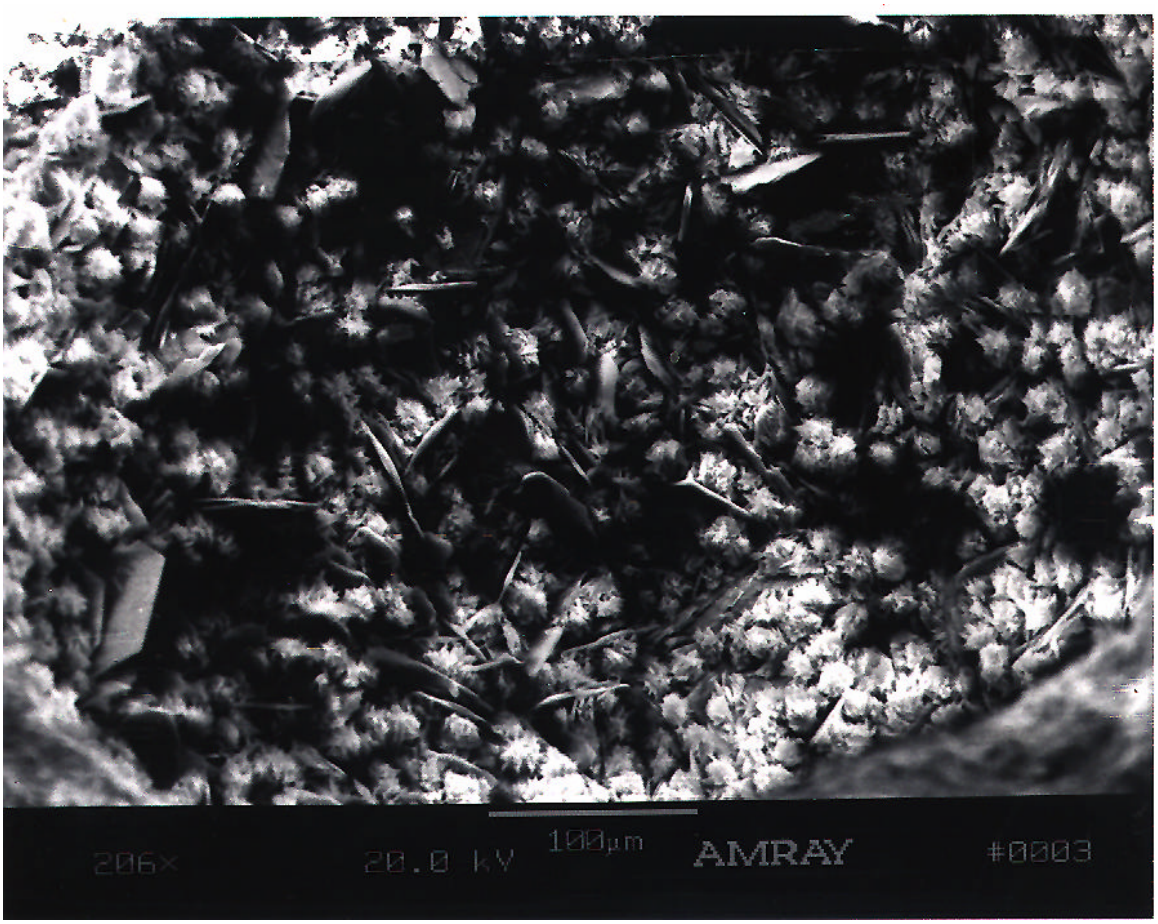

FIGURE 5.18 – Ettringite Bundles and Calcium Hydroxide Platelets

A wide view of ettringite bundles among calcium hydroxide platelets is shown above. The edges of Calcium hydroxide platelets distinctively form 120° angles. The site was found on an interior fragment of a submerged Silver Hill prism four (4) weeks after casting. The site is most likely a water void. No EDAX spectrum of this location is available. Probable identification of the suspected minerals is based on geometry and past experience examining concrete using the SEM.

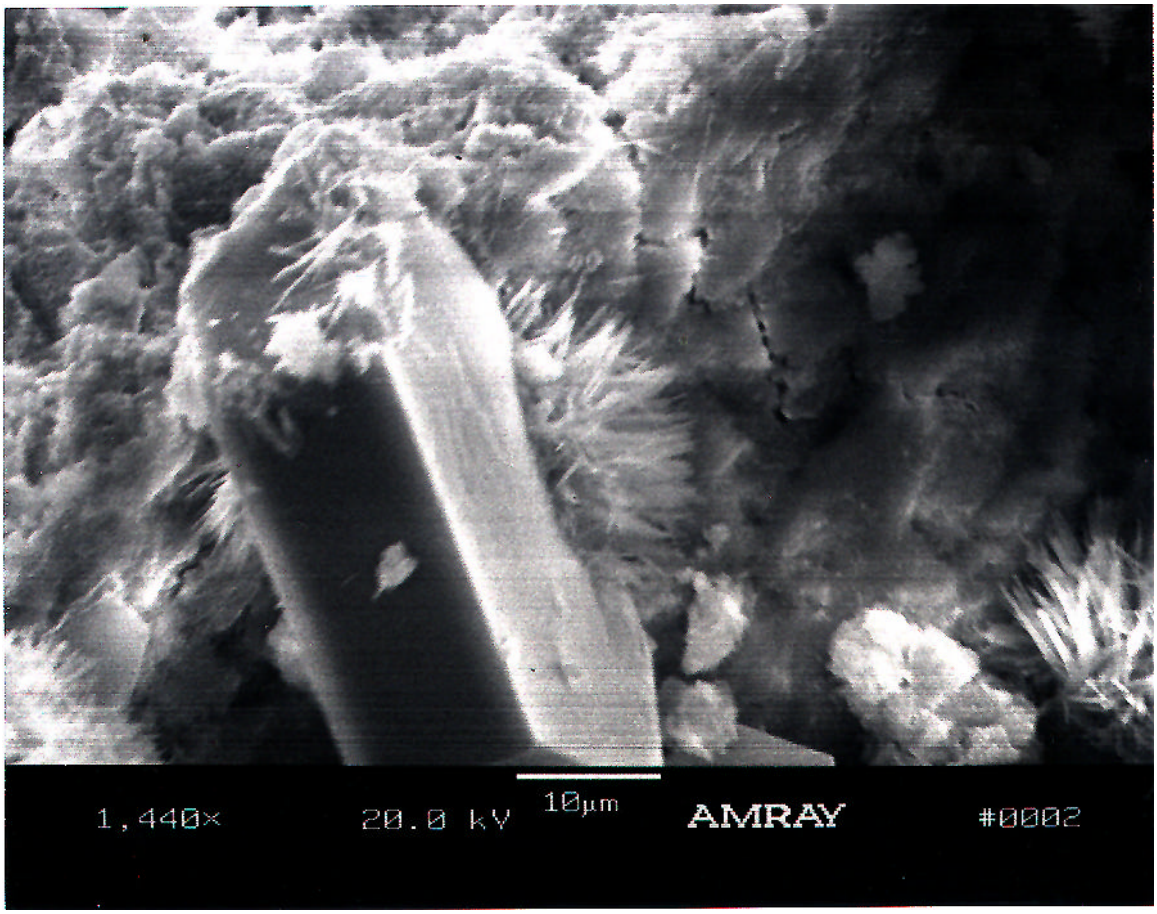

FIGURE 5.19– Ettringite Bundles, Calcium Hydroxide Platelets, and ASR Gel

Three points of interest identified above including a thick calcium hydroxide platelet surrounded by ettringite needles in the foreground. In the background and to the right were the crack is visible maybe the site of ASR. The photograph is of a interior fragment from a Silver Hill prism four (4) weeks after casting. The prism was stored under the submerged exposure condition.

FIGURE 5.20– Calcium Carbonate Exudates

A gel-like material was found exuding from the external cracks of most submerged prisms and cylinders. However, after drying, it was apparent the material was a powder and not a gel. Samples of the exudates were collected directly from the sides of the samples and investigated using the SEM. An EDAX spectrum (not shown) revealed that the powder was calcium based. The result seemed to indicate two possible identifications, calcium hydroxide or calcium carbonate, which are both products of cement hydration. An acid test was used to positively identify calcium carbonate, which reacts with hydrochloric acid, while excluding calcium hydroxide. The sample shown above was extracted from the exterior surface of a submerged Silver Hill prism nine (9) months after casting.

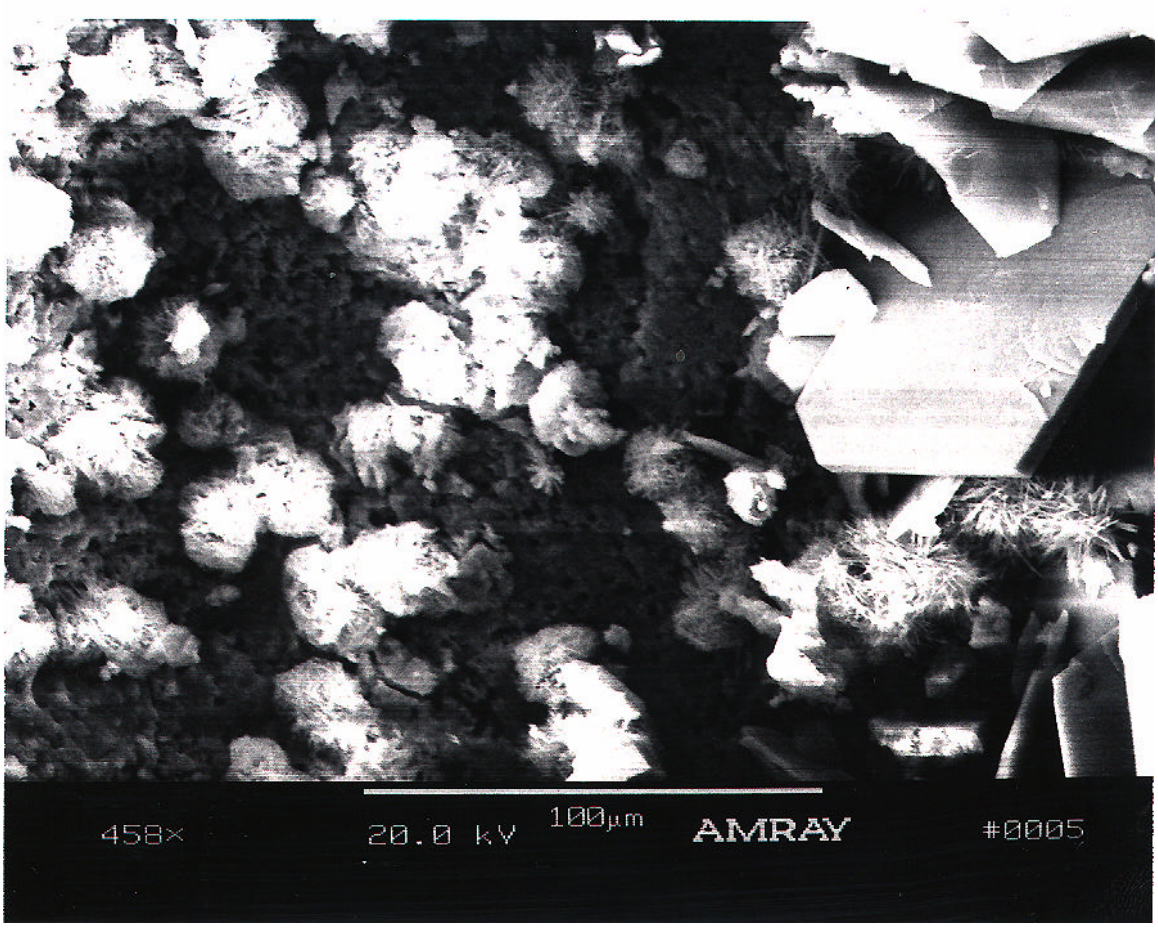

FIGURE 5.21– Ettringite and Calcium Hydroxide

The photograph above is of an interior fragment taken from a submerged Brandywine prism four (4) weeks after casting. Most likely the site is a water void (as opposed to air voids water voids are typically irregular and non-symmetrical).

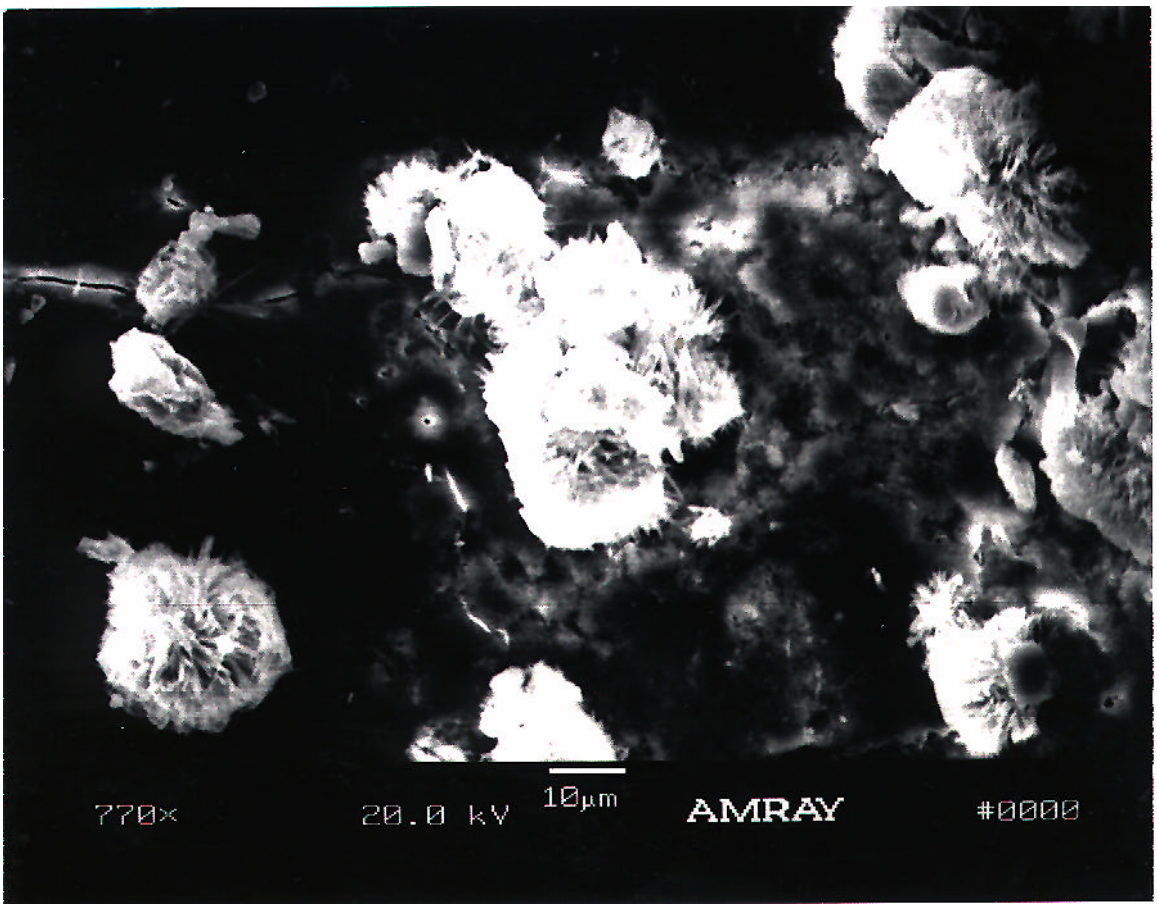

FIGURE 5.22– Ettringite and ASR Gel

Shown above are bundles of ettringite fibers in the foreground with possible ASR gel in the background. The site was located on an exterior fragment sampled from a submerged Silver Hill prism nine (9) months after casting.

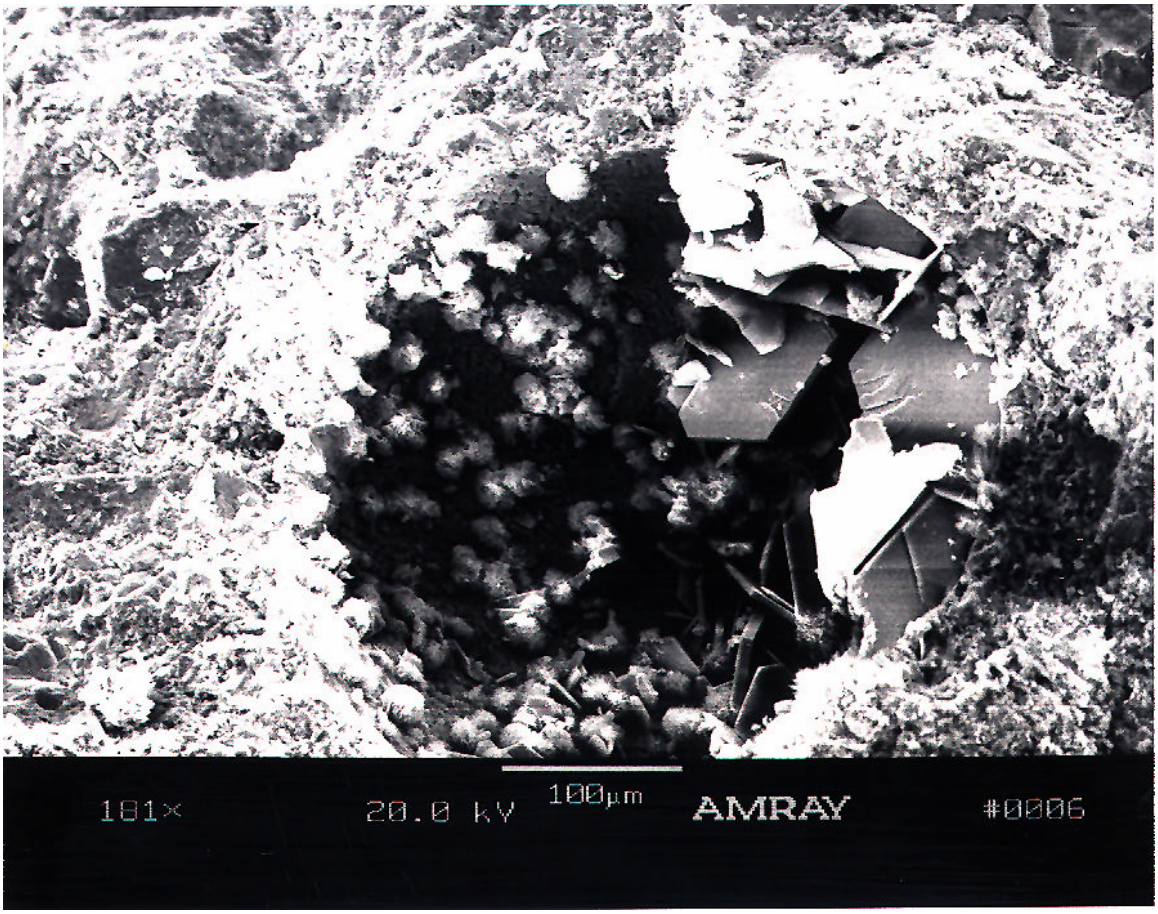

FIGURE 5.23– Ettringite and Calcium Hydroxide

A wide view of ettringite bundles among calcium hydroxide platelets is shown above. The site was found on an interior fragment of a submerged Millville prism four (4) weeks after casting. The site is an air void (symmetrical shape apparent in photograph).

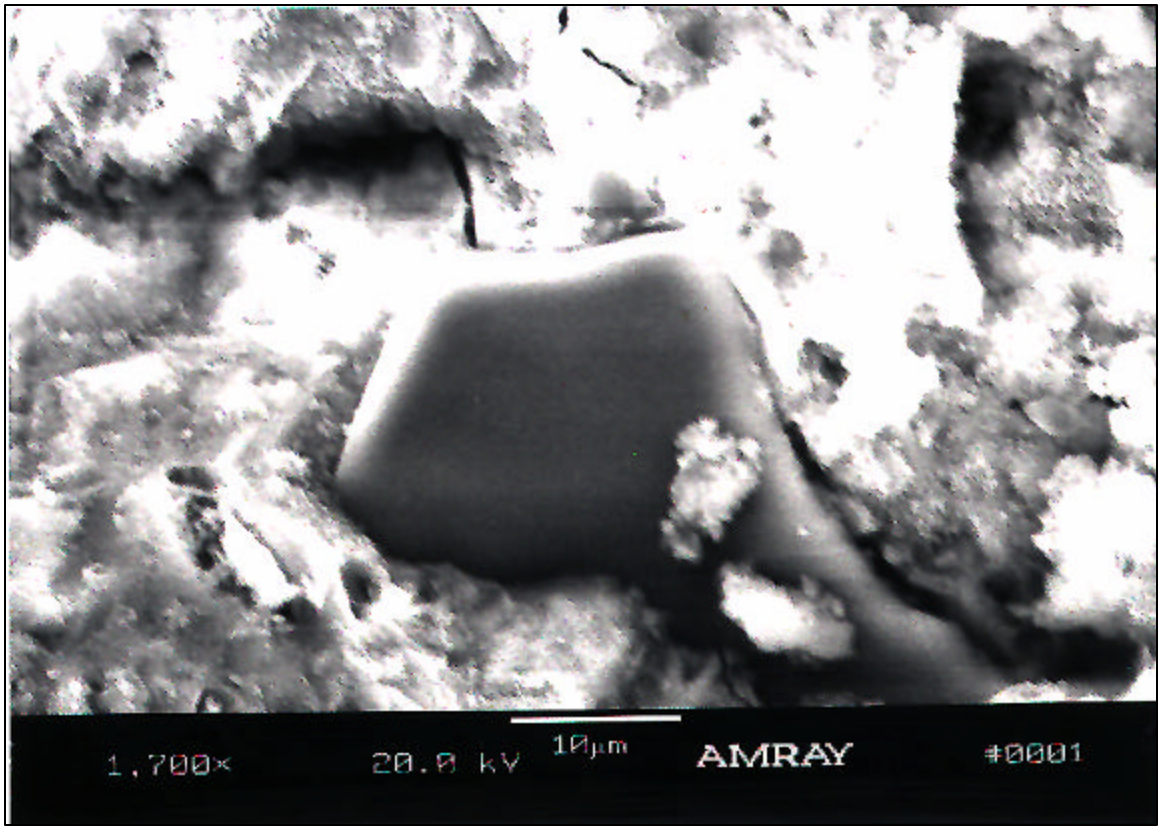

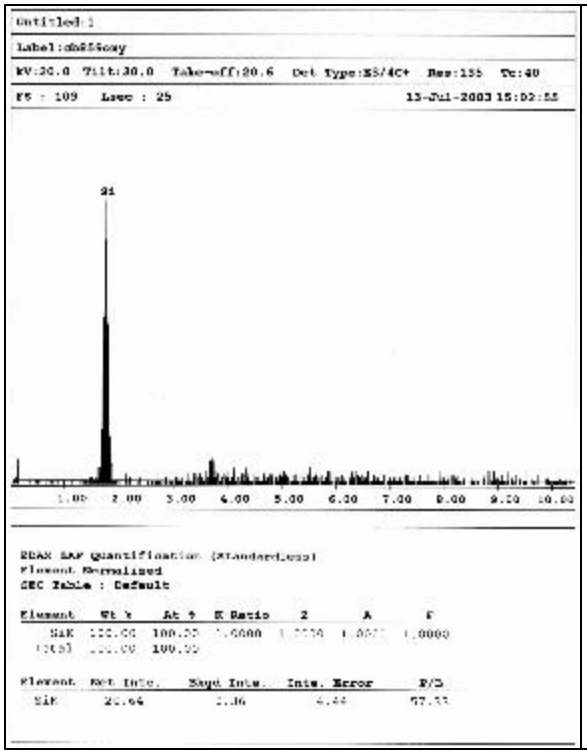

The photograph above and accompanying EDAX spectrum is of an interior fragment taken from a submerged Brandywine prism four (4) weeks after casting. The silicon peak is well defined. A peak to the left (unmarked in the photograph) is most likely an alkali such as potassium. To the right no discernable peak is present. The return is most likely background scattered noise, which is typical of a gel.

FIGURE 5.24– EDAX Identification of ASR Gel

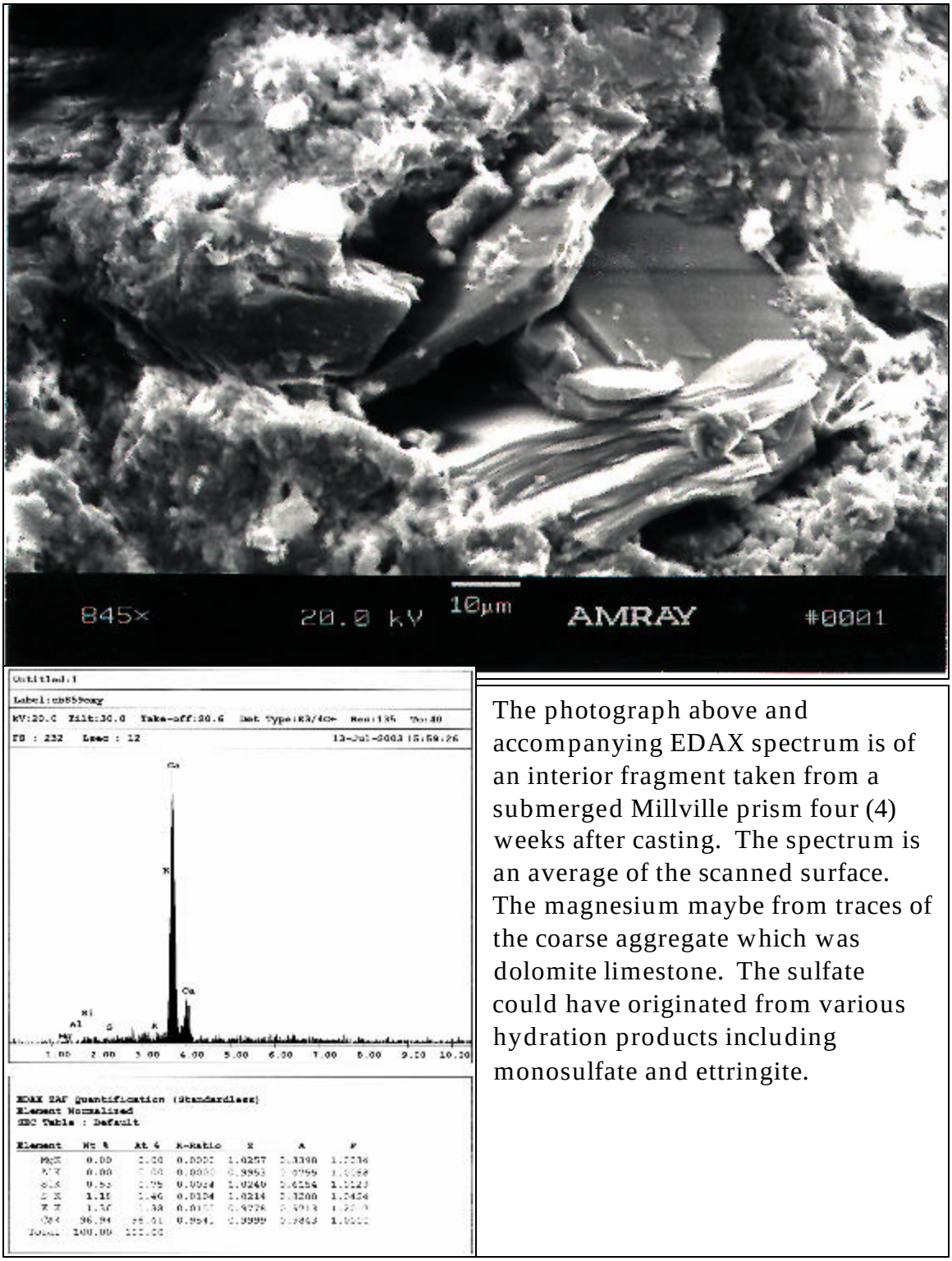

The photograph above and accompanying EDAX spectrum is of an interior fragment taken from a submerged Millville prism four (4) weeks after casting. The spectrum is an average of the scanned surface. The magnesium maybe from traces of the coarse aggregate which was dolomite limestone. The sulfate could have originated from various hydration products including monosulfate and ettringite.

FIGURE 5.25– EDAX Identification of Calcium Hydroxide

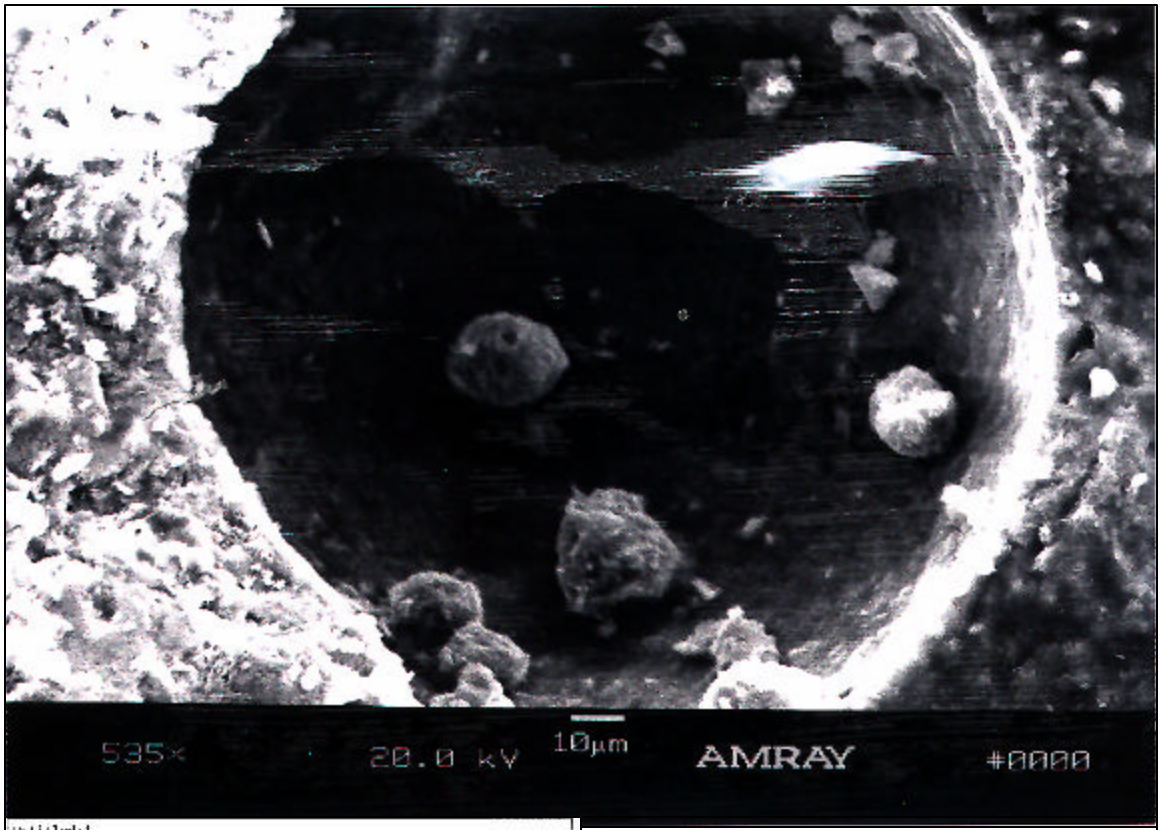

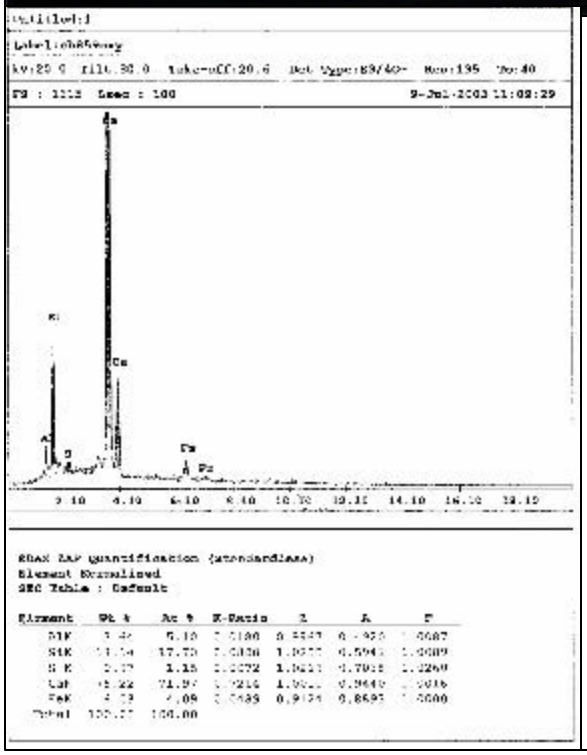

The photograph above and accompanying EDAX spectrum is of an interior fragment taken from a dry Brandywine prism four (4) weeks after casting. The spectrum is most likely of calcium silicate hydrate gel with other trace materials. To the right of the calcium peak, scattered background noise typical of gels was returned. The iron peaks could indicate traces of the coarse aggregate, which contained iron ore.

FIGURE 5.26– EDAX Identification of C – S – H Gel

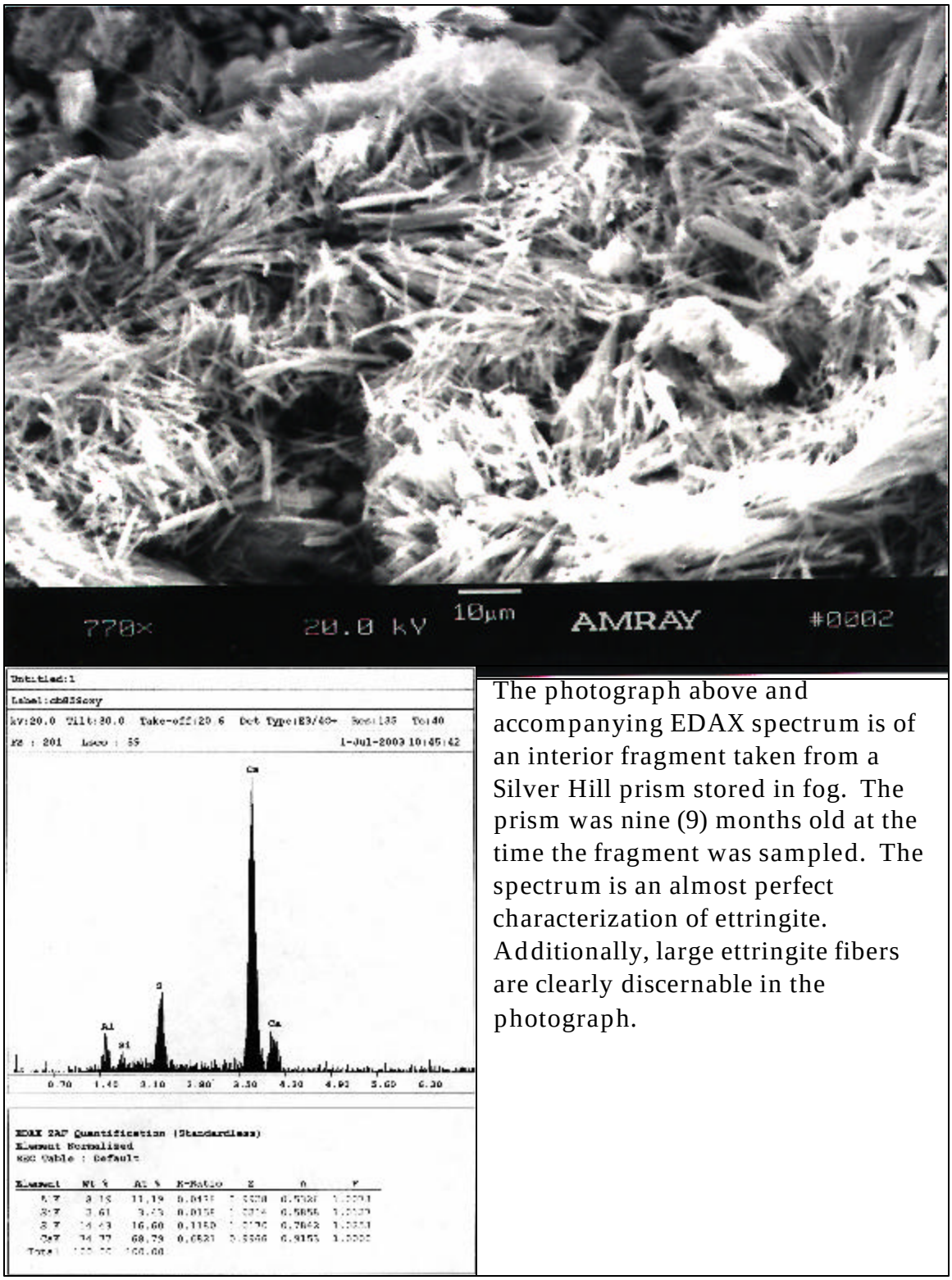

The photograph above and accompanying EDAX spectrum is of an interior fragment taken from a Silver Hill prism stored in fog. The prism was nine (9) months old at the time the fragment was sampled. The spectrum is an almost perfect characterization of ettringite. Additionally, large ettringite fibers are clearly discernable in the photograph.

FIGURE 5.27– EDAX Identification of Ettringite

CHAPTER 6 – Conclusions and Future Research Opportunities

6.1 Introduction

The implications of this research program's findings as they relate to the problem statement will be discussed. Also a connection between this study and previous research conducted by UMD/FHWA will be established. Finally, opportunities for further research building on this paper's findings are presented.

6.2 Research Program Goals and Accomplishments

This research program was designed to investigate the influence of fine aggregate lithology on DEF. It was noted that the sands selected for this study varied in several ways including geographic place of origin, method of production, and petrographic makeup. However, it was the role of the ASR expansiveness as defined by ASTM C1293 of each sand that was of particular interest to this study. Thus the study sought a connection between ASR and DEF. In theory, with all other factors being equal and only ASR reactivity among the fine aggregates as the variable, the interplay of ASR, delayed ettringite development, and expansion could be investigated in-depth.

This research program approached this investigation is several different ways. First, variables that could affect the behavior and chemistry of the concrete samples were diligently eliminated. For instance, a consistent and uniform cement sample was established, ASTM sampling methods were used to collect random fine aggregate samples, and only one coarse aggregate was used. Additionally, all concrete batches were designed for a 28-day compressive strength of 5,000 psi with 0.50 water-to-cement-ratio and 1.50% potassium level by weight of cement. Finally, all concrete samples underwent the same preparation sequence.

Other aspects of this study involved (1) the investigation of the Duggan Test method as modified by UMD/FHWA as a practical rapid expansion test for concrete samples (2) the impact of water exposure on the delayed formation and development of ettringite (3) the impact of fine aggregate type on the delayed formation and development of ettringite and (4) investigation of the expansion mechanism in concrete prisms. Conclusions drawn for each aspect of this study follow.

6.3 Effectiveness of Modified Duggan Test

Measurable expansion of the concrete prisms occurred within days of completing heat treatment by the Duggan Cycle. The heat treatment apparently initiated and accelerated the expansion mechanisms of the samples so that a process that would take years to complete in the field occurred within a matter of months.

During this research, weekly expansion measurements taken over a period of seven (7) months generated a unique expansion curve for each sample type. As demonstrated by the asymptotic nature of the curves, the expansion mechanisms had run their course within that seven (7) month period. Thus, the complete expansion curve could be used to identify individual processes involved in expansion.

The Modified Duggan Test, which uses prisms for linear length change measurements instead of the traditional cores, has the added advantage of not introducing cracks during the drilling of cores. Therefore, the internal crack patterns are left undisturbed for examination. This is critical since tracking the propagation of internal cracks could provide clues about the expansion behavior of the concrete. Additionally, using gauge stud inserts provides predefined and repeatable points on the prisms for making linear length change measurements.

6.4 Impact of Water Exposure on Ettringite Formation

This study finds that the amount of water exposure has a profound impact on delayed or secondary ettringite formation. While ettringite is a byproduct and will occur in concrete regardless of water exposure, the secondary development of ettringite is critically dependent on water.

To illustrate, the occurrence of ettringite in Millville samples at least hints at the crucial role of water on delayed ettringite development. Millville samples were the only sample set to include all three (3) exposure conditions. Millville is a non-reactive sand (0.028% ASR). Ettringite was found in the wet Millville samples but not in the dry. This of course does not mean that ettringite was not present in the dry samples. However, in qualitative terms, through a comprehensive SEM investigation of the samples, the conclusion can be made that ettringite was more developed in concentration and form in the wet samples; especially so in the submerged samples.

6.5 Impact of Fine Aggregate Type on Ettringite Formation

This study concludes that fine aggregate type can significantly predispose a sample to DEF and associated damaging expansion. Siliceous sand has been suspected in particular as a culprit (Azzam, 2002). Under this research program, Silver Hill was the only siliceous sand selected.

Additionally, fine aggregate type seemed to influence expansion more so than exposure condition. Samples made with Silver Hill sand consistently suffered greater expansion in terms of amount, rate, and duration despite exposure condition.

In qualitative terms, ettringite was easier to find using the SEM in samples made with Silver Hill sand. This conclusion is based on experience gained from a comprehensive examination of fractured surfaces.

6.6 Expansion Curves and Possible Expansion Mechanism

An analysis of the expansion curves using the first derivative plot identified three (3) regions and one (1) point of inflection on each curve. In each case, the initial expansion was followed by explosive expansion, which peaked about three (3) months after heat treatment by the Duggan Cycle. The maximum expansion rate was followed by a rapid decay in rate of expansion.

This study concludes the expansion curves are most likely the resultant of several expansion mechanisms. The interplay of the various mechanisms involved may vary as a function of time, thus producing the distinct regions observed on the expansion curves. Probable expansion mechanisms include the crystallization and growth of ettringite, expansion of ASR gel after absorption of water, and infiltration of water into the concrete matrix.

6.7 Links Found to Previous Research

The classical Kolmogorov-Avrami-Johnson-Mehl (KAJM) equation for nucleation and growth transformation has been used in the past to find coefficients for a mathematical model of concrete expansion (Livingston, 1998). Ramadan found good fit between the model and the first two hundred (200) days of expansion test data. The study concluded that the final model was the resultant of three (3) expansion phases: fast, intermediate, and slow. The lack of agreement between the model and long term expansion, after two hundred (200), maybe explained by the presence of a fourth very slow process. Ramadan et al. noted that the parameters of the model are empirically determined and may be dependant on the specific concrete mix and test conditions used (2004). Thus, the model needs to be applied to a wider range of concretes and test conditions to produce an empirical model that has general application.

Similarly, this study finds evidence supporting the interplay of several expansion mechanisms. In many cases, the expansion curves were asymptotic with one point of inflection. Three (3) regions on the expansion curve were

apparent. This could mean the mechanisms were involved in expansion to greater or lesser degree at the three (3) time intervals.

Prior studies have found factors, other than ASR, that contribute to ettringite development and expansion. The nature of the sand, differences in thermal expansion, aluminum content, and sand density all influence ettringite development and expansion in the concrete sample (Azzam 2002). These factors may explain the large expansion suffered by samples made with Silver Hill sand.

Though Silver Hill fine aggregate had a high rating on the mortar bar expansion test (0.28% by ASTM C1293), ASR gel was rarely found during the SEM investigation of fractured surfaces collected from that sample type. In fact, there was only one observed ASR gel particle. Thus, the expansion test, per ASTM C1293, does not necessarily measure the actual development of ASR.

6.8 Kinetics of the Expansion and the Damage Process

The expansions observed in this research program agreed with the ranking obtained in the MDSHA test: Silver Hill was the highest, Brandywine intermediate and Millville the lowest. This despite significant differences in the experimental procedures including the use of mortar bars in one case and concrete prisms in the other, and sodium hydroxide in the former and potassium carbonate in the other.

The aggregates were selected on the basis of their MDSHA expansion test ratings with the objective of covering the full range of values from low to high. As might be expected, the aggregates turned out to have very different lithologies, with the crushed limestone showing the least expansion. However, for the two siliceous aggregate types the expansion measurements did not predict the correct rank order of damage as measured by compressive strength at 270 days.

The kinetics of the expansion varied among the aggregates. It is important to examine the expansion rate curve, i.e. the time derivative of expansion, to characterize the process rather than relying solely on the measured expansion at some fixed point in time.

It is also worthwhile to conduct the expansion tests under more than one moisture storage condition. The various aggregates showed different responses to fog vs. submerged conditions. This suggests that the effect of each type of aggregate on the microstructure and hence the absorptivity of the cement paste needs to be considered in addition to its potential for ASR in evaluating expansion test data.

Ettringite was observed in most of the specimens. The morphology of the crystals may be an indication of the progress of damage. However, there is no quantitative way of correlating DEF with expansion measurements at the present time.

Finally, the results show that the measured expansions come from a combination of moisture absorption, DEF and ASR. Consequently, expansion tests do not measure ASR effects only.

6.9 Future Research

This research has provided some useful insights into the expansiveness of fine aggregates used by MDSHA. However, with only three different types of aggregates, it was not possible to investigate fully the influence of various factors such as mineralogy, grain-size distribution and method of manufacture. Therefore, this set of laboratory tests should be applied to additional fine aggregate types.

Since the lithology of an aggregate is associated with a given geological formation that is the result of specific geological processes, it may be possible to predict its expansiveness based on a knowledge of its geological origins.

Consequently, selection of additional fine aggregates should be designed to test this hypothesis.

The individual contributions of water absorption, DEF and ASR to the measured expansion needs to be clarified. This could include standard tests of permeability or absorptivity of concrete made with different fine aggregate types. The ASR reactivity of the fine aggregates alone could be measured by the modified ASTM C-289 test now being developed by the University of Illinois. Finally, a potential method for quantification of ettringite in concrete using 3-d synchrotron radiation is under development by FHWA and UMD through an NSF grant.

The role of the coarse aggregate needs to be established. Some researchers have proposed that the size of the aggregate is related to the observed thickness of the ettringite rims. Expansion tests on concrete specimens with different types and size distributions of coarse aggregate should be done to test this hypothesis.

The use of the Duggan heat cycle to induce microcracking makes it difficult to study the effect of high temperatures on the DEF process. Alternative methods of inducing microcracks such as fatigue cycles or focused sound waves needs to be evaluated.

The correlation between microcrack propagation damage and measured expansion could be determined using the nondestructive method of acoustic emissions (AE) (Ohtsu and Lida, 2001). The advantage of AE is that the measurements can be made continuously while the specimen is submerged. Moreover, it is possible to locate the position of the active cracks inside the specimen. Industrial computed tomography could be used to confirm the location and propagation of the cracks.

Finally, the relationship between ettringite crystal morphology and expansive stresses needs to be verified. This could be done by growing ettringite under controlled conditions in porous glass substrates.

ASTM STANDARDS

C 29 - Standards Test Method for Bulk Density ("Unit Weight") and Voids in Aggregate.

C 33 – Standard Specification for Concrete Aggregates.

C 39 – Standard Test Method for Compressive Strength of Cylindrical Specimens.

C 40 – Standard Test Method for Organic Impurities in Fine Aggregates for Concrete.

C 109 – Standard Test Method for Compressive Strength of Hydraulic Cement Mortars (Using 2-in. or 50-mm Cube Specimens).

C 125 – Standard Terminology Relating to Concrete and Concrete Aggregates.

C 138 – Standard Test Method for Unit Weight, Yield, and Air Content (Gravimetric) of Concrete.

C 192 – Standard Practice for Making and Curing Concrete Test Specimens in the Laboratory.

C 294 – Standard Descriptive Nomenclature for Constituents of Natural Mineral Aggregates.

C490 – Standard Practice for Use of Apparatus for the Determination of Length Change of Hardened Cement, Paste, Mortar, and Concrete.

C918 – Standard Test Method for Measuring Early-Age Compressive Strength and Projecting Later-Age Strength.

C1293 – Standard Test Method for Concrete Aggregates by Determination of Length Change of Concrete Due to Alkali-Silica Reaction.

D 75 – Standard Practice for Sampling Aggregates

D 3665 - Standard Practice for Random Sampling of Construction Materials

REFERENCES

Attiogbe, E.K., Wells, J.A. and Rizkalla, S.H., "Evaluation of Duggan Concrete Core Expansion Test," Research Report, Sponsored by Candian National Railways & Transport Institute, University of Manitoba, Winnipeg, Canada, September, 1990.

Azzam, A., Amde, A.M. and Livingston, R.A., "Delayed Ettringite Formation, The Effect of Fine Aggregate Type and Curing Conditions," Journal of Materials, ASCE (under review), 2004.

Berliner, R., "The Structure of Ettringite", Research Reactor Center, University of Missouri, Columbia, MO65211.

Collepardi, M., "Damage by Delayed Ettringite Formation," Concrete International, January, 1999, pp. 69 – 73.

Duggan, C.R. and Scott, J.F., "Proposed New Test for Alkali – Aggregate Reactivity," Canadian National Railways, Technical Research Report, Montreal, Canada, April 13, 1987, revised October 31, 1989.

Duggan, C.R. and Scott, J.F., "Establishment of New Acceptance / Rejection Limits for Proposed Test Method for Detection of Potientially Deleterious Expansion of Concrete," Presented to ASTM Subcommittee C09.02.02, September, 1989.

Johnson, D.M., Hooper, P.R. and Conrey, R.M., "XRF Analysis of Rocks and Minerals for Major and Trace Elements on a Single Low Dilution Li-tetraborate Fuse Bead," Advances in X-ray Analysis, Vol. 41, 1999, pp. 843-867.

Kosmatka, S. H. and Panarese, W.C., "Design and Control of Concrete Mixtures," Portland Cement Association, Skokie, Illinois.

Livingston, R.A., "Notes on Kologorov-Avrami-Johnson-Mehl Analysis of Modified Duggan Test Data," Unpublished Draft, Nov. 4, Turner-Fairbank Research Center, FHWA, 1998.

Livingston, R.A., “The Role of Potassium Hygric Cycling in Delayed Ettringite Formation,” Eleventh Annual V.M. Goldschmidt Conference, 2001.

Livingston, R.A., “The Damage Function Concept in the Deterioration Science of Concrete” Materials and Construction, (in press), 2004.

Marusin, S.L., “Sample Preparation – the Key to SEM Studies of Failed Concrete,” Cement & Concrete Composites, Vol. 17, 1995, pp 311-318.

Miller, F.M. and Tang, F.J., “The Distribution of Sulfur in Present-Day Clinkers of Variable Sulfur Content,” Cement and Concrete Research, Vol. 26, No. 12, 1996, pp. 1821-1829.

Ohtsu, M. and T. Iida, “Quantitative Damage Evaluation of Concrete Core Samples by Acoustic Emission,” Nondestructive Characterization of Materials X, R.E. Green, et al., Editors, Elsevier Science Ltd., 2001, pp. 257-264.

Pfeifer, D.W. and Marusin, S.L., “Energy Efficient Accelerated Curing of Concrete, a State – of - the - Art Review” Research Investigation by Wiss, Janney, Elstner & Associates, I11, for Prestressed Concrete Institute, Chicago, March, 1981.

Ramadan, E. O., Amde, A. M. and Livingston, R. A., "The Effect of Potassium and Initial Curing Concrete Expansion Associated with Delayed Ettringite Formation," ACI Materials Journal (under review), 2004.

Stark, J. and Bollmann, K., “Delayed Ettringite Formation in Concrete,” Bauhaus-University Weimar, Germany.

Stutzman, P.E., “Guide for X-ray Powder Diffraction Analysis of Portland Cement and Clinker,”NISTIR 5755, NIST, 1996.

Taylor, H.F.W., “Delayed Ettringite Formation”, Advances in Cement and Concrete, New Hampshire Conference, American Society of Civil Engineers, NY, 1994, pp. 121-131.

Thomas, M., “Delayed Ettringite Formation in Concrete: Recent Developments and Future Directions”, Materials Science of Concrete VI, S. Mindess and J. Skalny, Editors. American Ceramic Society: Westerville, OH. 2001, pp. 435-481.